Available online at www.sciencedirect.com

ScienceDirect

Nuclear Physics B 902 (2016) 354–386

NUCLEAR PHYSICS B

www.elsevier.com/locate/nuclphysb

Finite size spectrum of $SU(N)$ principal chiral field from discrete Hirota dynamics

Vladimir Kazakov [a,b,1], Sébastien Leurent [a,c,d,*]

[a] *Ecole Normale Superieure, LPT, 75231 Paris Cedex-5, France*
[b] *Université Paris-VI, Paris, France*
[c] *Imperial College, London SW7 2AZ, United Kingdom*
[d] *Institut de Mathématiques de Bourgogne, UMR 5584 du CNRS, Université de Bourgogne-Franche-Comté, 9 avenue Alain Savary, 21000 Dijon, France*

Received 9 June 2015; accepted 11 November 2015

Available online 18 November 2015

Editor: Stephan Stieberger

Abstract

Using recently proposed method of discrete Hirota dynamics for integrable $(1+1)$D quantum field theories on a finite space circle of length L we derive and test numerically a finite system of nonlinear integral equations for the exact spectrum of energies of $SU(N) \times SU(N)$ principal chiral field model as functions of mL, where m is the mass scale. We propose a determinant solution of the underlying Y-system, or Hirota equation, in terms of Wronskian determinants of $N \times N$ matrices parameterized by $N-1$ functions of the spectral parameter θ with the known analytic properties at finite L. Although the method works in principle for any state, the explicit equations are written for states in the $U(1)$ sector only. For $N > 2$, we encounter and clarify a few subtleties in these equations related to the presence of bound states, absent in the previously considered $N=2$ case. As a demonstration of efficiency of our method, we solve these equations numerically for a few low-lying states at $N=3$ in a wide range of mL.

* Corresponding author.
E-mail addresses: kazakov@lpt.ens.fr (V. Kazakov), sebastien.leurent@nsup.org (S. Leurent).
[1] Member of Institut Universitaire de France.

http://dx.doi.org/10.1016/j.nuclphysb.2015.11.012
0550-3213/

1. Introduction

Integrable $1+1$ dimensional quantum field theories on a finite space circle have been rather intensively studied in the last 20 years [1–10]. A great deal of success in the exact treatment of the finite size effects in various integrable QFT's was due to the thermodynamic Bethe ansatz (TBA) approach [11] resulting in a system (in most of the cases infinite) of non-linear integral equations. It was realized that the TBA equations could be rewritten in a functional, Y-system form [2].

Recently, a novel, quite general approach to these problems was proposed in [12] based on the integrability of the Y-system. The Y-system is known to be a gauge invariant version of the famous Hirota bilinear equation, often called the T-system, in its discrete form [13]. The underlying discrete Hirota dynamics is integrable and general solutions of Hirota equations can be found in a determinant (Wronskian) form [14] for various boundary conditions corresponding to a variety of different problems, from matrix models to quantum spin chains and quantum sigma-models. For finite rank symmetry groups, the Wronskians contains only a finite number of functions of the spectral parameter. Thus the Wronskian solution can drastically simplify the problem: the infinite Y-system is reduced to a finite number of non-linear integral equations for these functions. Then the subtlest point comes: We should guess the analytic properties of these functions w.r.t. the spectral parameter. This is relatively easy to do for the spin chains where the polynomiality of transfer matrix leads to the final answer in terms of a set of Bethe ansatz equations. For the QFT's at a finite volume L (length of the space circle) the situation is much more complicated and the analyticity properties of the Y-functions are not so obvious. Nevertheless, it often appears to be possible to extract them, partially from physical considerations, partially from certain assumptions of the absence of unphysical singularities. It helps to transform the Y-system into a system of non-linear integral equations (NLIE), more tractable, and better suitable for the numerical studies. The resulting equations can remind the Destri–De Vega NLIE [1] or even coincide with them for a limited set of 2D QFT's where these DDV equations are known.

This program was first performed in [12] for the $SU(2)_L \times SU(2)_R$ principal chiral field (PCF) for a general quantum state, and the numerical study of the finite size spectrum was successfully done for a variety of interesting states, from the vacuum and mass-gap to quite general states, in the so called $U(1)$ sector or even lying out of it (i.e. having excitations in left and right $SU(2)$ spin modes).

In this paper, we will construct within these lines the corresponding NLIE's for $SU(N) \times SU(N)$ PCF at any N. We use the Wronskian solution of [14] for the underlying Hirota equation in terms of determinants of $N \times N$ matrices and guess the correct analytic form of the functions entering the Wronskian. For the vacuum state, the asymptotic Bethe ansatz (ABA) based on the scattering theory and, strictly speaking, valid only for sufficiently large length L teaches us that there are no singularities on the physical strip of the rapidity plane, at least for not too small L's.[2]

For excited states there are certain poles entering the physical strip, and their qualitative structure can be guessed from the ABA. The explicit construction is done only for states in the $U(1)$ sector, but we sketch out the generalization to any state. We show how the exact S-matrix of the model (including the CDD factor) naturally emerges from this approach based on the Y-system by simple analyticity assumptions.

[2] This argument based on ABA cannot exclude a possibility that at a sufficiently small size, some extra singularities occur. However, our numerics give serious evidence that at least for $N = 3$ such extra singularities do not appear.

The presence of additional singularities on the physical strip related to the bound states, absent for $N = 2$, leads in the $N > 2$ case to significant modifications, already in the expression for the energies of excited states. We find from our NLIE's the finite size (Lüscher) corrections which reveal the presence of the so called μ-terms. We also test our NLIE's analytically, comparing the results with the known analytic data in the ultraviolet (conformal) limit. Finally, we demonstrate the power of our approach by solving the resulting NLIE's numerically, for the vacuum energy and the energies of some low lying excited states as functions of the size mL for $N = 3$.

One of the principal motivations for our work was the possibility to realize the same program in the case of recently constructed AdS/CFT Y-system [15–17] for the exact spectrum of anomalous dimensions in $N = 4$ supersymmetric Yang–Mills theory. The PCF model, having $N - 1$ particles (including $N - 2$ bound states) in its asymptotic spectrum, bears many similarities with the AdS/CFT case where the number of bound states is infinite. The corresponding Wronskian solutions of AdS/CFT Y-system, or Hirota equation with the so called T-hook boundary conditions is also available [18,19].

2. The principal chiral field model in the large volume

In this section we will give the definition of the PCF model, remind the reader the basics of scattering theory for the physical particles and the ABA equations, and describe the equations for the finite size spectrum in terms of the Y-system.

2.1. The PCF model, its S-matrix and the large L ABA

The $SU(N) \times SU(N)$ PCF model has the classical action

$$\mathcal{S}_{\text{PCF}} = -\frac{1}{2\,e_0^2}\int d\tau \int_0^L d\sigma\, \mathrm{tr}[(h^{-1}\partial_\alpha h)^2]\,, \qquad h(\sigma,\tau) \in SU(N)\,. \tag{1}$$

The spectrum of this asymptotically free theory in the infinite volume $L \to \infty$ consists of $N - 1$ physical particles with masses

$$m_a = m\,\frac{\sin\frac{\pi a}{N}}{\sin\frac{\pi}{N}} \tag{2}$$

where the lowest mass scales with the bare charge e_0 according to the asymptotic freedom $m = \frac{\Lambda}{e_0} e^{-\frac{4\pi}{N e_0^2}}$ (Λ is a cut-off). Its wave function transforms in the fundamental representation under each of the $SU(N)$ subgroups. The exact S-matrix for bi-fundamental particles, found from the conditions of factorizability, crossing, unitarity, analyticity and the bound state structure [20], reads[3] [21,22]:

$$\hat{S}_{12}(\theta) = \breve{\chi}_{CDD}(\theta)\cdot S_0(\theta)\frac{\hat{R}_{L,R}(\theta)}{\theta - i} \otimes S_0(\theta)\frac{\hat{R}_{L,R}(\theta)}{\theta - i} \tag{3}$$

$$S_0(\theta) = \frac{\Gamma\left(i\frac{\theta}{N}\right)\Gamma\left(\frac{1-i\theta}{N}\right)}{\Gamma\left(-i\frac{\theta}{N}\right)\Gamma\left(\frac{1+i\theta}{N}\right)}\,, \qquad \breve{\chi}_{CDD} = \frac{\sinh(\pi\theta/N + i\pi/N)}{\sinh(\pi\theta/N - i\pi/N)} \tag{4}$$

[3] In the $N = 2$ case, these definitions give $\breve{\chi}_{CDD} = -1$ corresponding to the multiplication of S_0 by i.

where we introduced the standard $SU(N)$ R-matrix $\hat{R}_{L,R}(\theta) = \theta + i\hat{P}_{L,R}$ and $\hat{P}$ is the permutation operator exchanging the left/right spins of the scattering particles. In particular, crossing and unitarity lead to the following identity

$$\prod_{k=-\frac{N-1}{2}}^{\frac{N-1}{2}} S_0(\theta + ik) = -\frac{\theta - i\frac{N-1}{2}}{\theta + i\frac{N-1}{2}} \tag{5}$$

on the scalar (dressing) factor.

We can use this S-matrix to study the spectrum of $\mathcal{N}$ particles on a periodic space circle of a sufficiently big circumference $L \gg m^{-1}$ imposing periodicity of the wave function

$$\prod_{j=k+1}^{\mathcal{N}} \hat{\mathcal{S}}(\theta_k - \theta_j) \prod_{j=1}^{k-1} \hat{\mathcal{S}}(\theta_k - \theta_j)|\Psi\rangle = e^{-imL\sinh(2\pi\theta_k/N)}|\Psi\rangle\,, \tag{6}$$

which quantizes the momenta of the physical particles. The asymptotic spectrum is then given by

$$E \simeq \sum_{j=1}^{\mathcal{N}} m\cosh\left(\frac{2\pi}{N}\theta_j\right) + O(e^{-mL}) \tag{7}$$

where θ_j are given by solutions to the system of nested Bethe equations following from the diagonalization of (6). This diagonalization can be performed by means of the algebraic Bethe ansatz and leads to the asymptotic Bethe ansatz (ABA) equations (43) and (32) [23,24].[4]

We will rederive the ABA equations as a large L limit of the Y-system of the model – a system of equations valid at any finite volume L and presented in the next subsection. Eq. (43) represents the diagonalized version of the periodicity condition (6). Eq. (32) is the set of $2(N-1)$ nested Bethe equations for the auxiliary right and left magnon roots $u_j^{(k)}$ and $v_j^{(k)}$ following from a regularity condition, as we will see in section 4.1.

Note that the ABA equations (32) remind the Bethe ansatz equations for two inhomogeneous $SU(N)$ spin chains with the inhomogeneity parameters θ_j given by the rapidities of physical particles. Their dynamics is defined by the periodicity equation (43). So the large L limit can be also called the "spin chain limit".

2.2. TBA, Y-system and Hirota equation

The generalization of the ABA equations to any length L is achieved by the TBA trick [2]: the system is put on the space time torus, with a finite space period L and a big Euclidean "time" period $R \to \infty$. Then, using the relativistic invariance, we exchange the roles of time and space and solve the problem for the same system but rather with the infinite space extent R with a periodic "time" L which can be interpreted as the inverse temperature [25]. The full energy spectrum of such an infinite system can be found from the nested BAE (6) and from (7) by means of the so called string hypothesis. The resulting equations for the densities of bound states are presented in [26], following the direct solution of the PCF given in [27] (see also [28]).

[4] In what follows we will measure all dimensional quantities in the units of the mass m, so that we put everywhere $m = 1$. The only continuous parameter of the problem is now the volume L.

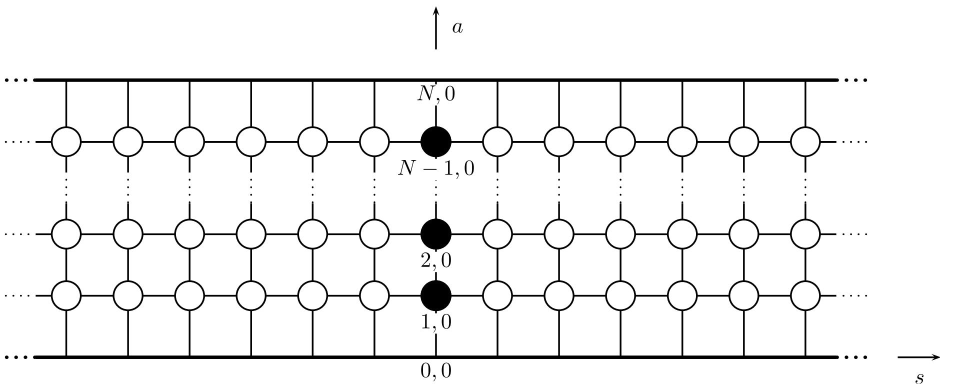

Fig. 1. The (a, s)-strip for Y-system and T-system.

The free energy calculation at a finite temperature for such an infinite volume system can be done thermodynamically, using the saddle point approximation due to [29]. Then the resulting integral TBA equations can be rearranged into the Y-system[5]

$$Y^+_{a,s}\,Y^-_{a,s} = \frac{1+Y_{a,s+1}}{1+(Y_{a+1,s})^{-1}}\frac{1+Y_{a,s-1}}{1+(Y_{a-1,s})^{-1}}, \qquad a = 1, 2, \ldots, N-1; \quad -\infty < s < \infty \tag{8}$$

where, by definition, $Y_{0,s} = Y_{N,s} = \infty$ and we have the following[6] boundary conditions at $\theta \to \pm\infty$:

$$Y_{a,s} \sim e^{-Lp_a(\theta)\delta_{s,0}} \times \text{const}_{a,s}\,, \qquad p_a = \cosh(\frac{2\theta\pi}{N})\frac{\sin(\frac{a\pi}{N})}{\sin(\frac{\pi}{N})}\,. \tag{9}$$

This Y-system describing PCF at finite L is an infinite set of functional equations (8) with the functions $Y_{a,s}(\theta)$ of the spectral parameter θ defined in the nodes marked by black and white bullets in the interior of the infinite strip in a, s lattice represented in Fig. 1.

A direct but rather tedious derivation of this Y-system was performed in Appendix A of [12] for $N = 2$. The generalization of this calculation to $N > 2$ is rather straightforward, but the Y-system (8) is known from other considerations [30] and is a very universal system of equations describing the integrable Hirota dynamics [14].

As we will see later, the expression for the momentum $p_a(\theta)$ is the only one compatible with the Y-system and relativistic invariance, up to a normalization that can be absorbed into the definition of the size L of the spin chain.[7] As a result of (9) we see that the middle node Y-functions, $Y_{a,0}$, $a = 1, 2, \cdots, N-1$, are exponentially suppressed at large L or at large $|\theta|$.

Obviously, the Y-system (8) has many solutions and to specify the physical solution we have to describe its analytic properties. To have a qualitative idea of the analyticity we have to consider a certain limit for the solution where we know the corresponding Y-functions entirely as analytic

[5] To make many formulas less bulky, the shifts of the spectral parameter will be often denoted as follows $f^\pm = f(\theta \pm \frac{i}{2})$, $f^{\pm\pm} = f(\theta \pm i)$, and in general $f^{[\pm k]} = f(\theta \pm \frac{i}{2}k)$.

[6] Note that the notation p_a refers to the auxiliary model where the roles of space and time are exchanged; in the original model, it corresponds rather to an energy.

[7] So that the length L is actually measured in units of mass.

functions of the spectral parameter θ. The most convenient limit is $L \to \infty$ where we can solve the Y-system directly, with the appropriate physically natural analyticity assumptions, to obtain explicitly all Y-functions and make a link with the exact scattering matrix and the resulting ABA equations, as it was done for the $N = 2$ case in [12]. We will give this asymptotic solution in section 4. Then the Y-system, in the form of TBA equations, can be in principle solved numerically by iterations, starting at large L and then adiabatically approaching $L \sim 1$, and even very small L's corresponding to the ultraviolet CFT behavior. The method was successfully used for various integrable sigma models, including the $SU(2)$ PCF [12,31,32,7]. It will be also the main method of this paper devoted to the $SU(N)$ PCF for $N > 2$. For the vacuum state, the information from ABA is trivial: it suggests that we don't have any singularities in the physical strip $-iN/4 < \mathrm{Im}(\theta) < iN/4$, at least for not too small L's, since there are no Bethe roots.[8]

The TBA procedure described above leads to the following expression for the vacuum energy

$$E_{vacuum}(L) = -\frac{m}{N}\sum_{a=1}^{N-1}\frac{\sin(\frac{a\pi}{N})}{\sin(\frac{\pi}{N})}\int_{-\infty}^{\infty} d\theta\cosh\left(\frac{2\pi}{N}\theta\right)\log\left(1+Y_{a,0}(\theta)\right). \tag{10}$$

With certain modifications in the analytic properties of Y-functions, described in the next section, the equations (8)–(10) appear to be appropriate not only for the vacuum state, as it was originally derived from the string hypothesis, but also for the excited states [3,4]. Y-functions for various excited states differ by their analytic properties which can be qualitatively inferred, as it was mentioned above, from the same states in the ABA. A naive heuristic proposal which worked well for the $N = 2$ case is that the excited states correspond to the appearance of logarithmic poles in the integrand of (10) at the points θ_j where

$$Y_{1,0}(\theta_j + iN/4) + 1 = 0. \tag{11}$$

If the contour is deformed so that it encircles these singularities, the pole calculation will give a contribution $\sum_{j=1}^{\mathcal{N}} m\cosh\frac{2\pi\theta_j}{N}$ which fits well the prediction of the ABA formula (7). However, the situation appears to be more complicated at $N \geq 3$, already because of the fact that unlike the $N = 2$ case of [12], the solutions θ_j of (11) are not necessarily real and this naive prescription should be slightly modified in order to get a real energy. This will be explained in detail in section 5. One should admit that the right formulas for energies of excited states in the integrable sigma-models are still rather a matter of a natural guess then of a reliable derivation. More insight is needed into this issue.

To solve the Y-system equation (8) we will often use it in the form of the Hirota equation

$$T^+_{a,s}T^-_{a,s} = T_{a+1,s}T_{a-1,s} + T_{a,s+1}T_{a,s-1} \tag{12}$$

on a set $\{T_{a,s}\}$ of functions of the spectral parameter θ related to the original Y-functions as follows

$$Y_{a,s} = \frac{T_{a,s+1}T_{a,s-1}}{T_{a+1,s}T_{a-1,s}}. \tag{13}$$

On the boundary, one sets $T_{a,s} = 0$ if $a \notin \{0, 1, \ldots, N\}$, so that T-functions are associated to the nodes of the grid in Fig. 1, including the boundaries $a \in \{0, N\}$.

[8] It does not guarantee that we will not have some singularities entering the physical strip when L becomes small enough. But our numerical result doesn't suggest such a strange behavior.

The Hirota equation (12) is invariant under the gauge transformation

$$T_{a,s} \to \chi_1^{[a+s]} \chi_2^{[a-s]} \chi_3^{[-a+s]} \chi_4^{[-a-s]} T_{a,s} \tag{14}$$

so that T-functions are gauge dependent, whether as Y-functions (13) are gauge invariant. Another useful relation following from (12) is

$$1 + Y_{a,s} = \frac{T_{a,s}^+ T_{a,s}^-}{T_{a+1,s} T_{a-1,s}} \,. \tag{15}$$

3. Central node equations

The central node Y-functions $Y_{a,0}$ related to the black, momentum carrying nodes in Fig. 1 play a special role in the Y-system. It will be useful for the future to solve the corresponding Y-system equations for these functions entering the l.h.s. of (8) in terms of the r.h.s.

Let us rewrite the Y-system (8) in the form

$$\frac{Y_{a,s}^+ Y_{a,s}^-}{\left(Y_{a+1,s}\right)^{1-\delta_{a,N-1}} \left(Y_{a-1,s}\right)^{1-\delta_{a,1}}} = \frac{1 + Y_{a,s+1}}{\left(1 + Y_{a+1,s}\right)^{1-\delta_{a,N-1}}} \frac{1 + Y_{a,s-1}}{\left(1 + Y_{a-1,s}\right)^{1-\delta_{a,1}}} \,. \tag{16}$$

At $s = 0$ it can be rewritten using (13)–(15) as follows

$$Y_{a,0}^{\star\Delta} = \frac{T_{a,1}^{\star\Delta} (T^{(L)})_{a,-1}^{\star\Delta}}{T_{a+1,0}^{\star\Delta} T_{a-1,0}^{\star\Delta}} \times \left(\frac{T_{N,0}^+ T_{N,0}^-}{T_{N,1} T_{N,-1}^{(L)}} \right)^{\delta_{a,N-1}} \left(\frac{T_{0,0}^+ T_{0,0}^-}{T_{0,1} T_{0,-1}^{(L)}} \right)^{\delta_{a,1}} \tag{17}$$

where we introduced a discrete D'Alembert operator Δ on the interval $a \in [1, N-1]$ defined by the formula[9]

$$F_a^{\star\Delta} := \frac{F_a^+ F_a^-}{\left(F_{a+1}\right)^{1-\delta_{a,N-1}} \left(F_{a-1}\right)^{1-\delta_{a,1}}} \tag{18}$$

for any function $F_a(\theta)$, and δ is the Kronecker symbol, used to add the counter terms necessary to satisfy (16) even at $a = 1$ and $a = N - 1$. By a superscript (L) in $T_{a,-1}^{(L)}$ in (17) we denoted a T-function in a gauge of a type (L) which can be different from the gauge of the other T-functions in that formula. We can do so because $1 + Y_{a,s} = \frac{(T_{a,s})^{\star\Delta}}{T_{0,s}^{\delta_{a,1}} T_{N,s}^{\delta_{a,N-1}}}$ in the right hand side of (16) are gauge invariant, and we are allowed to write each Y-function in terms of T's taken in a different gauge. The meaning and the notation of the gauge (L) will be explained later.

We can act by Δ^{-1} on both sides of (17), to get

$$Y_{a,0} = e^{-L p_a(\theta)} \frac{T_{a,1} T_{a,-1}^{(L)}}{T_{a+1,0} T_{a-1,0}} \left(\left(\frac{T_{N,0}^+ T_{N,0}^-}{T_{N,1} T_{N,-1}^{(L)}} \right)^{\delta_{a,N-1}} \left(\frac{T_{0,0}^+ T_{0,0}^-}{T_{0,1} T_{0,-1}^{(L)}} \right)^{\delta_{a,1}} \right)^{\star\Delta^{-1}} \tag{19}$$

where $p_a = \cosh(\frac{2\theta\pi}{N}) \sin(\frac{a\pi}{N}) / \sin(\frac{\pi}{N})$. The factor $e^{-L p_a(\theta)}$ is a zero mode of Δ, in the sense that $\left(e^{-L p_a(\theta)}\right)^{\star\Delta} = 1$, and it is added in order to reproduce the asymptotics (9). This equation (19) is valid up to a zero mode, which will be discussed in the next sections, though we can

[9] The terming "discrete D'Alembert operator" becomes clear if one takes the logarithm of the r.h.s. and the l.h.s. of (18).

already see that this remaining zero-mode has a constant asymptotics at large θ. Furthermore, the action of the operator Δ^{-1} can be easily calculated by the discrete Fourier transform in θ, a variables, so that the final expression is

$$Y_{a,0} = e^{-Lp_a(\theta)} \frac{T_{a,1} T^{(L)}_{a,-1}}{T_{a+1,0} T_{a-1,0}} \left(\mathbf{\Pi}_{N-a} \left[\frac{T^+_{0,0} T^-_{0,0}}{T_{0,1} T^{(L)}_{0,-1}} \right] \mathbf{\Pi}_a \left[\frac{T^+_{N,0} T^-_{N,0}}{T_{N,1} T^{(L)}_{N,-1}} \right] \right)^{\star K_N}, \tag{20}$$

$$\text{where } f^{\star K_N} = e^{\log f \star K_N}, \tag{21}$$

and $\star$ stands for convolution; the "fusion" operator $\mathbf{\Pi}_s$ is defined as the following product

$$\mathbf{\Pi}_k[f](\theta) = \prod_{j=-(k-1)/2}^{(k-1)/2} f(\theta + i\, j) = f^{[-k+1]} f^{[-k+3]} \dots f^{[k-3]} f^{[k-1]} \tag{22}$$

and the kernel K_N is the operator inverse to $\mathbf{\Pi}_N$: $\forall f$ regular, $(\mathbf{\Pi}_N[f])^{\star K_N} = f$. Its Fourier transform is

$$\widetilde{K_N}(\omega) = \frac{1}{\sum_{j=-\frac{N-1}{2}}^{\frac{N-1}{2}} e^{2i\pi j \omega}}. \tag{23}$$

Back in the θ-space it takes the form

$$\begin{aligned} K_N(\theta) &= \frac{1}{2N} \left[\tan\left(\frac{\pi - 2\pi i \theta}{2N} \right) + \tan\left(\frac{\pi + 2\pi i \theta}{2N} \right) \right] \\ &= \frac{1}{N} \frac{\sin(\pi/N)}{\cosh(2\pi\theta/N) + \cos(\pi/N)}. \end{aligned} \tag{24}$$

4. The large L, "spin chain" limit of Y-system and its relation to ABA

We will derive in this section the large L, ABA equations (43), (32) directly from the Y-system (8). Following the logic of [12] we use the fact that the Y-functions of the momentum carrying (black) nodes are exponentially small in this limit:

$$Y_{a,0} = \frac{T_{a,1} T_{a,-1}}{T_{a+1,0} T_{a-1,0}} \sim e^{-Lp_a(\theta)}. \tag{25}$$

This implies that the two wings, left (for $s < 0$) and right (for $s > 0$), of the Y-system (8) are almost decoupled and can be treated separately.

4.1. Expressions for T-functions in the large volume, spin chain limit

Eq. (25) suggests that either $T_{a,1} \sim e^{-Lp_a(\theta)}$ or $T_{a,-1} \sim e^{-Lp_a(\theta)}$. Which one does so (whereas another one is finite) is a matter of choice of a gauge for T-functions.

We will work with two different gauges (R) and (L), such that in the large L limit we have

$$\underbrace{T^{(R)}_{a,-1} \ll 1 \qquad , T^{(L)}_{a,1} \ll 1}_{1 \le a \le N-1} \qquad , T^{(R)}_{a,s\ge 0} \sim 1 \qquad , T^{(L)}_{a,s\le 0} \sim 1 \tag{26}$$

(R) will be called the "right-wing-gauge" and (L) the "left-wing-gauge", and when this superscript will be omitted it will be implicitly assumed that we are working in the (R) gauge.

In the large L limit, the T-functions of the left (L) and right (R) gauge both describe the same Y functions but (up to exponential corrections) they satisfy Hirota equation restricted to the wings $s \geq 0$ (resp. $s \leq 0$). Moreover, these T-functions are in this limit analytic on the whole complex plane, and therefore polynomial.

Such a solution of Hirota equation is well known in applications to the fusion procedure in similar spin chain systems, bosonic [14] or even supersymmetric [33,34]. First we parameterize $T_{1,s}$ in terms of N functions $X^{(W)}_{(j)}(\theta)$, $j = 1, \dots, N$ by means of the following generating functional

$$\hat{W}^{(W)} = \left(1 - X^{(W)}_{(N)}(\theta)\, e^{i\partial_\theta}\right)^{-1} \left(1 - X^{(W)}_{(N-1)}(\theta)\, e^{i\partial_\theta}\right)^{-1} \dots \left(1 - X^{(W)}_{(1)}(\theta)\, e^{i\partial_\theta}\right)^{-1}$$
$$= \sum_{s=0}^{\infty} \frac{T^{(W)}_{1,\pm s}(\theta + \frac{i}{2}(s-1))}{\varphi(\theta - N\frac{i}{4})} e^{is\partial_\theta} \tag{27}$$

where the superscript $W = R, L$ indicates the wing that we study (either right or left), and $\pm s$ is equal to s for the right wing (if $W = R$) and to $-s$ for the left wing (if $W = L$).

These functions $X^{(W)}_{(j)}(\theta)$ can be further expressed as follows

$$X^{(W)}_{(k)} = \frac{Q^{(W)\,[N/2-k-1]}_{k-1}}{Q^{(W)\,[N/2-k+1]}_{k-1}} \frac{Q^{(W)\,[N/2-k+2]}_{k}}{Q^{(W)\,[N/2-k]}_{k}}, \quad k = 1, 2, \dots, N \tag{28}$$

in terms of some Q-functions[10] denoted as $Q^{(W)}$. These Q functions in the corresponding gauge are polynomials characterizing different solutions of Hirota equation in the large L limit, their roots are the Bethe roots describing various excited states – solutions of the Y-system[11]:

$$Q^{(R)}_k(\theta) = \prod_{j=1}^{J^{(R)}_k} \left(\theta - u^{(k)}_j\right), \quad Q^{(L)}_k(\theta) = \prod_{j=1}^{J^{(L)}_k} \left(\theta - v^{(k)}_j\right) \quad (k = 1, \cdots, N-1) \tag{29}$$

$$Q^{(R,L)}_N(\theta) \equiv \varphi(\theta) = \prod_{j=1}^{\mathcal{N}} (\theta - \theta_j), \qquad Q^{(R,L)}_0(\theta) \equiv 1\,. \tag{30}$$

In particular, we have from (27)

$$T^{(W)}_{1,\pm 1}(\theta) = \varphi(\theta - \frac{iN}{4}) \sum_{k=1}^{N} X^{(W)}_{(k)}(\theta)\,. \tag{31}$$

$T_{1,\pm 1}$ should be free of poles, i.e. polynomial. But for each Bethe root $w_j = u^{(k)}_j$ or $w_j = v^{(k)}_j$, the two functions $X^{(W)}_{(k)}$ and $X^{(W)}_{(k-1)}$ have a pole at the same position $w_j - \frac{i}{2}\left(\frac{N}{2} - k\right)$. By requiring their cancellation in the sum (31), we get a constraint on the position of w_j, which we will call the auxiliary Bethe equation:

10 The present Q-functions Q_k correspond to the functions $Q_{1,2,\dots,k}$ in the Hasse diagram notation of [35].

11 We assume here that there exists a gauge such that the large L limit is described by polynomial functions $Q^{(W)}_k$. Although it needs a better understanding from the point of view of Y-system, it is the case if we start treating the large L limit from the S-matrix by the ABA approach.

$$-1 = \frac{Q_{k-1}^{(R/L)}(w_j - i/2)}{Q_{k-1}^{(R/L)}(w_j + i/2)} \frac{Q_k^{(R/L)}(w_j + i) Q_{k+1}^{(R/L)}(w_j - i/2)}{Q_k^{(R/L)}(w_j - i) Q_{k+1}^{(R/L)}(w_j + i/2)},$$
$$\text{where } \begin{cases} k = 1, 2, \ldots, N-1 \\ w_j = u_j^{(k)} \text{ resp. } v_j^{(k)} \end{cases} \tag{32}$$

The rest of the T-functions in the right wing can be expressed through the Cherednik–Bazhanov–Reshetikhin (CBR) determinant[12] [36,37]

$$T_{a,s} = \frac{\det_{1 \le j,k \le a} T_{1,s+k-j}\left(\theta + \frac{i}{2}(a+1-k-j)\right)}{\mathbf{\Pi}_{a-1}\left[\varphi^{[\mp s - N/2]}\right]} \tag{33}$$

and they are also automatically polynomial in virtue of (32).

Among these Q-functions, the polynomial function $Q_N = \varphi$, encoding, as its roots, the rapidities of all physical particles, will be of a particular importance, and the vanishing of $T_{a,-1}^{(R)}$ or $T_{a,1}^{(L)}$ due to (25) implies the following asymptotics[13]

$$\varphi(\theta) = \lim_{L\to\infty} T_{a,0}^{(R,L)}(\theta + i\frac{N-2a}{4}) \tag{34}$$

$$= \lim_{L\to\infty} T_{0,s>0}^{(R)}(\theta + i\frac{N+2s}{4}) = \lim_{L\to\infty} T_{0,s<0}^{(L)}(\theta + i\frac{N-2s}{4}) \tag{35}$$

$$= \lim_{L\to\infty} T_{N,s>0}^{(R)}(\theta - i\frac{N+2s}{4}) = \lim_{L\to\infty} T_{N,s<0}^{(L)}(\theta - i\frac{N-2s}{4}) \tag{36}$$

These relations translate all the zeroes θ_j of $Y_{1,0}(\theta + i\frac{N}{4}) + 1$, giving the roots of Bethe equation (11), into the zeroes of T-functions.

4.2. Asymptotic Bethe ansatz (ABA)

Now we will reproduce from the Y-system in large volume limit $L \to \infty$ the ABA equations (43), (32) for the spectrum of energies. In this spin chain limit, (20) can be employed to compute $Y_{a,0}$ to the leading order, by using the asymptotic behaviors (26).

At this point, it is interesting to notice that the crossing relation (5) implies that up to a zero mode of $\mathbf{\Pi}_N$ (i.e. up to a function Z such that $\mathbf{\Pi}_N[Z] = 1$)[14]

$$\left(\frac{\varphi^+}{\varphi^-}\right)^{\star K_N} = \frac{\varphi^{[+2-N]}}{\varphi^{[-N]}}\left(\frac{\varphi^{[-2N+1]}}{\varphi^-}\right)^{\star K_N} = \frac{\varphi^{[+2-N]} S^{[-N]}}{\varphi^{[-N]}} = \frac{\varphi^{[+N]} S^{[+N]}}{\varphi^{[-2+N]}} \tag{37}$$

$$\text{where} \quad S(\theta) := \prod_j S_0(\theta - \theta_j) \quad \text{i.e.} \quad S = (-1)^{\mathcal{N}/N}\left(\frac{\varphi^{[-N+1]}}{\varphi^{[+N-1]}}\right)^{\star K_N}. \tag{38}$$

---

12 Equation (33) makes sense if $a \ge 1$, and can be extended to $a = 0$ under natural conventions: one can use the convention that $\mathbf{\Pi}_{-a}[f] = 1/\mathbf{\Pi}_a[f]$ – consistently with $\mathbf{\Pi}_{a+1}[f] = f^{[a]}\mathbf{\Pi}_a[f^-]$ – and that the determinant of the empty matrix is equal to one, so that at $a = 0$ the relation (33) reduces to $T_{0,s} = \varphi^{[\mp s - N/2]}$.

Also note that the sign of the shift in the denominator $\varphi^{[\mp s - N/2]}$ is different for $T^{(R)}$ and $T^{(L)}$. This sign is actually a convention which can be fixed using the gauge freedom (14).

13 The statement in (34) is a bit too strong and we will see further that it actually only holds inside some strips on the complex plane.

14 One can note that the sign $(-1)^{1/N} = e^{i(2k+1)\pi/N}$ is defined up to a factor $e^{i2k\pi/N}$, which is a zero mode of $\mathbf{\Pi}_N$ and can be ignored.

By denoting[15] $\varepsilon = (-1)^{\mathcal{N}/N}$, this gives for instance

$$\lim_{L\to\infty} \mathbf{\Pi}_{N-a}\left[\frac{T^+_{0,0}T^-_{0,0}}{T_{0,1}\cdot T^{(L)}_{0,-1}}\right]^{\star K_N} = \mathbf{\Pi}_{N-a}\left[\frac{\varphi^{[-N/2+1]}}{\varphi^{[-N/2-1]}}\right]^{\star K_N} = \mathbf{\Pi}_{N-a}\left[\varepsilon\frac{\varphi^{[+N/2]}S^{[+N/2]}}{\varphi^{[-2+N/2]}}\right]$$

$$= \frac{\varphi^{[3N/2-a-1]}}{\varphi^{[-N/2+a-1]}}\,\mathbf{\Pi}_{N-a}\left[\varepsilon S^{[+N/2]}\right] \tag{39}$$

$$= \frac{\varphi^{[3N/2-a-1]}}{\varphi^{[-N/2+a-1]}}\frac{\varphi^{[-N/2-a+1]}}{\varphi^{[3N/2-a-1]}}\frac{1}{\mathbf{\Pi}_a\left[\varepsilon S^{[-N/2]}\right]}. \tag{40}$$

As a consequence, the large L limit of equation (20) is

$$Y_{a,0}(\theta) \sim e^{-Lp_a}\frac{T_{a,1}T^{(L)}_{a,-1}}{T_{a+1,0}T_{a-1,0}}\frac{\varphi^{[-N/2-a+1]}}{\varphi^{[-N/2+a-1]}}\frac{\varphi^{[-N/2-a+1]}}{\varphi^{[-N/2+a+1]}}\frac{1}{\mathbf{\Pi}_a\left[\left(S^{[-N/2]}\right)^2\chi^{[-N/2]}_{CDD}\right]}, \tag{41}$$

$$\text{where } \chi_{CDD}(\theta) := \prod_j \breve{\chi}_{CDD}(\theta-\theta_j)\,. \tag{42}$$

Here, the factor χ_{CDD} (4) was added as another zero mode, necessary to transform the double poles and double zeroes of S^2 into the simple ones [22]. We will also see in section 7.3.2 that this factor arises in our Y-system formalism in a natural way.

In particular, at $a = 1$, we get the ABA equation (periodicity condition for the wave function):

$$-1 = e^{-iL\sinh\frac{2\pi}{N}\theta_j}\frac{1}{\chi_{CDD}(\theta_j)S(\theta_j)^2}\frac{Q^{(L)}_{N-1}(\theta_j-i/2)}{Q^{(L)}_{N-1}(\theta_j+i/2)}\frac{Q^{(R)}_{N-1}(\theta_j-i/2)}{Q^{(R)}_{N-1}(\theta_j+i/2)} \tag{43}$$

which expresses the fact that $Y_{1,0}(\theta_j + iN/4) + 1 = 0$ (here $T_{1,1}$ was replaced by the single surviving, last term of (31)).

In conclusion, we have shown here that the Y system implies the familiar ABA equations [26,22]. In the next sections we will see how these ABA equations for the spectrum of PCF can be generalized to any finite size L.

5. Expressions for the energy of excited states

No complete and full proof procedure is known to generalize the formula (10) to the excited states.[16] The analytic continuation of [4] with respect to the mass is difficult, if possible at all for a general state in our model. The procedure of [4,8] claims that for the excited states a set of logarithmic poles (different for each state) appears under the integral in (10). From (34) and the ABA we know that at very large L, $T_{a,0}(\theta) \simeq \varphi(\theta - iN/4 + ia/2)$, where $\varphi(\theta) = \prod_j(\theta-\theta_j)$ is a polynomial encoding all *real* roots[17] For finite L the roots θ_j will be shifted and in general become complex. These exact Bethe roots, as opposed to the approximate ones given by (43), are defined by the exact Bethe equations $T_{a,0}(\theta^{(a)}_j + iN/4 - ia/2) = 0$. There is a whole family of such roots when $a \in [0, N]$, because even though the two functions $T_{a,0}(\theta)$ and $T_{a+1,0}(\theta - i/2)$

[15] One can note that $\varepsilon^2 = (-1)^{2\mathcal{N}/N}$ is a zero mode of $\mathbf{\Pi}_N$, which is ignored as long as we work up to a zero mode.

[16] Except for the $N = 2$ case where we know from [12] the complete description of all excited states.

[17] We consider here for simplicity only the situation when the Bethe roots θ_j are real in the asymptotic limit. The case when they occur in complex conjugated pairs should not be very different but at the moment we did not try to do it.

have the same limit at large L, they do not necessarily have the same roots at finite size. Each of these roots also gives rise to two zeroes and two poles in the Y-functions, namely, as we see from (15), $1 + Y_{a,0}(\theta_j^{(a)} + iN/4 - ia/2 \pm i/2) = 0$ and $1 + Y_{a\pm 1,0}(\theta_j^{(a)} + iN/4 - ia/2) = \infty$. Among these families of finite size Bethe roots, we will actually restrict ourselves to the roots $\theta_j^{(\frac{N}{2})}$ for even N, and $\theta_j^{(\frac{N\pm 1}{2})}$ for odd N. We will argue that only those ones will contribute as poles caught by an integration contour.

Separating the logarithmic poles (where $1 + Y_a$ cancels) in the contour integral (10) should give a familiar contribution $\sum_j \cosh \frac{2\pi}{N}\theta_j$ to the energy of a finite L state. This appears to be the right, though not completely well understood and justified, answer for some models, including the PCF at $N = 2$ [12].

For PCF at $N > 2$ this procedure encounters another difficulty: the zeros under the logarithm in (10) appear to correspond in general to complex Bethe roots θ_j. We have to decide what is the right integration contour in (10) when this formula is applied to an excited state. We are not aware of any well justified procedure for fixing the contour but we shall try to guess it on the basis of our numerical observations and the symmetry considerations.

In the rest of this section, we consider the formula for excited states of the $U(1)$ sector – the one which corresponds to the wave function $|\Psi\rangle$ having the maximal value of total spin $S_L = S_R = \mathcal{N}/2$ w.r.t. the $SU(N)_R$ and $SU(N)_L$ symmetries. In this case $J_k^{(L,R)} = 0$ and there are no auxiliary roots in the ABA Q-functions (29) (all of them are equal to 1 except $Q_N^{(R,L)} = \varphi$, see (29)–(30)). In what follows, we shall distinguish even and odd N's.

5.1. Energy of state in the $U(1)$ sector at odd N's

It is believed that the energy of an excited state can be obtained from (10) by an analytic continuation in the parameter L. This continuation has the effect of appearance of new singularities of the integrand in the physical strip in (10) and a certain choice of the integration contour, enclosing some singularities of the integrand [3,4]. How it happens in each particular model or state is usually a rather complicated question. It implies the analysis of positions of these singularities at a finite L but the large L asymptotics often serves as an important guiding principle.

Here we propose a formula for the energies of excited states in the $U(1)$ sector which seems to work well for any odd N. It is based on our numerical and analytic observations, in particular for the $N = 3$ case. It reads as follows

$$E(L) = -\frac{m}{N}\sum_{a=1}^{N-1}\frac{\sin(\frac{a\pi}{N})}{\sin(\frac{\pi}{N})}\int\limits_{-\infty-N\frac{i}{4}+a\frac{i}{2}}^{\infty-N\frac{i}{4}+a\frac{i}{2}} \mathrm{d}\theta\ \cosh\left(\frac{2\pi}{N}\theta\right)\log\left(1+Y_{a,0}(\theta)\right) \tag{44}$$

so that we have the straight integration contours parallel to the real axis and shifted by $-N\frac{i}{4} + a\frac{i}{2}$.[18]

Let us explain the reason for such a choice of contours. First, let us note that in order to have a real energy from (44) we should impose the following property of Y-functions under

[18] One of the advantages of this straight contour is that it can be easily implemented in numerics. We will see indeed that the Y functions can be most easily computed on exactly these lines. We will also see that the statement holds only for roots with even momentum number, but for odd momentum number, the (slightly modified) contour stays very close to this straight line.

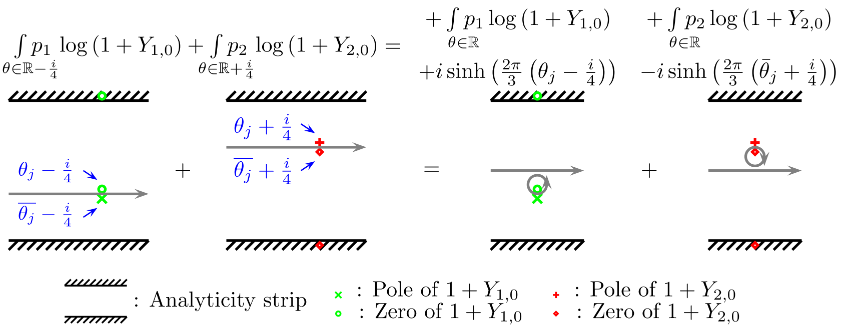

Fig. 2. Analyticity of the integrand $\cosh(\frac{2\pi}{3}\theta)\log\left((1+Y_{1,0})(1+Y_{2,0})\right)$ and manipulations with the contours when $N=3$.

complex-conjugation: $\overline{Y_{a,s}(\theta)} = Y_{N-a,s}(\bar\theta)$. We will restrict ourselves to the gauges where this property is a consequence of the relation

$$\overline{T_{a,s}(\theta)} = T_{N-a,s}(\bar\theta) \tag{45}$$

For finite L, we will focus on the roots θ_j defined[19] by $T_{\frac{N-1}{2},0}(\theta_j + i/4) = 0$.

Due to the very definition of $1 + Y_{a,0} = \frac{T^+_{a,0}T^-_{a,0}}{T_{a+1,0}T_{a-1,0}}$, each θ_j gives rise to two zeros and poles. In particular, $1 + Y_{\frac{N-1}{2},0}(\theta)$ has a zero and a pole[20] at respective positions $\theta_j - i/4$ and $\overline{\theta_j} - i/4$ because $T^+_{\frac{N-1}{2},0}(\theta_j - i/4) = 0$ and $T_{\frac{N+1}{2},0}(\overline{\theta_j} - i/4) = 0$. In the large L limit these zero and pole almost coincide since θ_j is almost real. By complex conjugation, we can also say that $1 + Y_{\frac{N+1}{2},0}(\theta)$ has a zero and a pole at respective positions $\bar\theta_j + i/4$ and $\theta_j + i/4$.

This structure is illustrated for $N = 3$ in Fig. 2. From the Lüscher corrections,[21] we can say that the pole occurs below the zero for $1 + Y_{1,0}$ and vice versa for $1 + Y_{2,0}$, at least for roots with even momentum numbers.[22] This is important to ensure the right answer if we want the contours to be straight.

In (44) we chose the integration contour to pass, for the $\frac{N-1}{2}$ and $\frac{N+1}{2}$-th term in the sum, between those zero and pole. Deforming the contour to the real axis and computing the contributions of the logarithmic poles enclosed by the contour during that deformation,[23] one gets the following formula

$$E(L) = -\frac{m}{N}\sum_{a=1}^{N-1}\frac{\sin(\frac{a\pi}{N})}{\sin(\frac{\pi}{N})}\int_{-\infty}^{\infty} d\theta \cosh\left(\frac{2\pi}{N}\theta\right)\log\left(1 + Y_{a,0}(\theta)\right)$$

19 In this section, we will denote θ_j for $\theta_j^{(\frac{N-1}{2})}$, because the other types of finite size roots don't contribute.

20 In addition to this zero and pole, $1 + Y_{\frac{N-1}{2},0}(\theta)$ has another zero at $\theta_j + 3i/4$ and a pole at each root of $T_{\frac{N-3}{2},0}$, but this will not have any consequence in the contour argument.

21 In section 8.1, we detail how this is proved in the asymptotic limit. Our numerics suggests that it is still true at finite size, and even in the conformal limit.

22 So that the contour will actually have to be slightly modified for roots having odd momentum number. This will be done in such a manner that (46) will stay true.

23 The contour deformation is best understood after an integration by parts which removes logarithmic cuts and changes the cosh into a sinh.

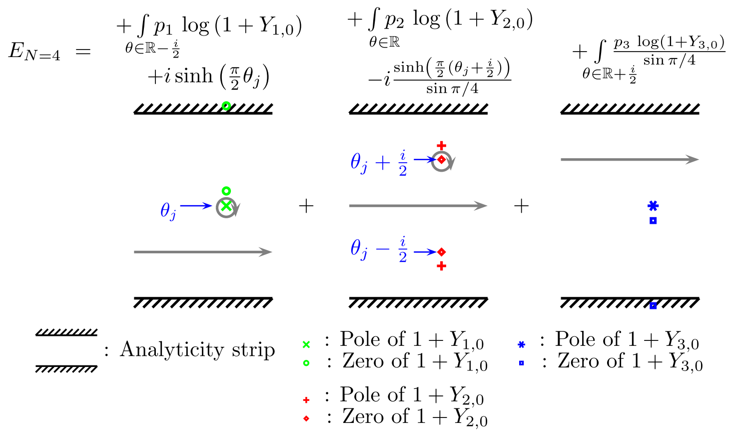

Fig. 3. Analyticity of the integrand for the energy and choice of the contours for $N = 4$.

$$+i\sum_j m\frac{\cos\frac{\pi}{2N}}{\sin\frac{\pi}{N}}\left[\sinh\left(\frac{2\pi}{N}(\theta_j - i/4)\right) - \sinh\left(\frac{2\pi}{N}(\bar{\theta}_j + i/4)\right)\right] \tag{46}$$

In the thermodynamic limit ($L \gg 1$), the Bethe roots θ_j become real and the second line of (46) reduces to the asymptotic result (7), whereas the term in the first line appears to be $O(e^{-mL})$.

5.2. *Energy of state in the $U(1)$ sector at even N's*

When N is even, the corresponding contour cannot be chosen as a straight line. We will conjecture here the analogue of (46) to be simply

$$E(L) = -\frac{m}{N}\sum_{a=1}^{N-1}\int_{-\infty-N\frac{i}{4}+a\frac{i}{2}}^{\infty-N\frac{i}{4}+a\frac{i}{2}} p_a(\theta)\log\left(1+Y_{a,0}(\theta)\right)\mathrm{d}\theta \;+\sum_j \cosh(\theta_j) \tag{47}$$

where the roots θ_j are defined by $T_{\frac{N}{2},0}(\theta_j) = 0$, so that the second term in (47) is real due to the reality of $T_{\frac{N}{2},0}$. The corresponding contour is shown in Fig. 3.

We should admit here that this formula for the masses at even N has a status of a natural conjecture. We have not enough of numerical, or analytic evidence to be 100% sure in it. It would be good to verify it at least for the mass gap at $N = 4$, numerically and by means of the Lüscher corrections at large L.

6. Wronskian solution for Hirota equation equivalent to Y-system

For the principal chiral field, $T_{a,s}$ is defined for $a = 0, 1, \ldots, N$, while $Y_{a,s}$ is defined for $a = 1, 2, \ldots, N-1$. We can solve the Hirota finite difference equation (12) (and the corresponding Y-system) with the appropriate boundary conditions using its integrability. Any solution of (12) is gauge equivalent to a solution where $T_{0,s}(\theta) = T_{0,0}(\theta - s\frac{i}{2})$ and $T_{N,s}(\theta) = T_{N,0}(\theta + s\frac{i}{2})$. We will choose this convention for the gauge $T^{(R)}$:

$$T^{(R)}_{0,s}(\theta) = T^{(R)}_{0,0}(\theta - s\frac{i}{2}), \quad \text{and} \quad T^{(R)}_{N,s}(\theta) = T^{(R)}_{N,0}(\theta + s\frac{i}{2}). \tag{48}$$

The most general solution under this gauge constraint can be expressed [14] as an $N \times N$ determinant, in terms of $2N$ unknown functions q_j and $\overline{q_j}$[24,25]:

$$T^{(R)}_{a,s}(\theta) = i^{\frac{N(N-1)}{2}} \mathrm{Det}(c_{j,k})_{1\le j,k\le N} \tag{49}$$

$$\text{where} \qquad c_{j,k} = \overline{q_j}\left(\theta + \frac{i}{2}\left(s + a + 1 + \frac{N}{2} - 2k\right)\right) \quad \text{if } k \le a$$

$$\text{and} \qquad c_{j,k} = q_j\left(\theta + \frac{i}{2}\left(-s + a + 1 + \frac{N}{2} - 2k\right)\right) \quad \text{if } k > a\,.$$

At this point, q_j is not necessarily the complex-conjugate of $\overline{q_j}$ and the gauge freedom reduces to two independent functions g and $\bar{g}$

$$q_j(\theta) \to g(\theta)\cdot q_j(\theta) \tag{50}$$

$$\overline{q_j}(\theta) \to \bar{g}(\theta)\cdot \overline{q_j}(\theta) \tag{51}$$

As an example of this determinant solution, the large L (spin chain limit) solution corresponding to the states of $U(1)$ sector, described by the roots θ_i, can be easily identified by plugging the following values for q_j into (49)

$$q_j(\theta) = \overline{q_j}(\theta) = \frac{\theta^{j-1}}{(j-1)!} \quad \text{for } 1 \le j < N$$

$$q_N(\theta) = \overline{q_N}(\theta) = P_\infty(\theta) \tag{52}$$

$$\text{where } (i\, e^{-\frac{i}{2}\partial_\theta} - i\, e^{\frac{i}{2}\partial_\theta})^{N-1} P_\infty = \varphi = \prod_k (\theta - \theta_k) \tag{53}$$

To see that this is the correct parameterization of the $U(1)$ solution, first, we can convince ourselves that $T_{a,-1} = 0$, $T_{a,0} = \varphi(\theta - i\frac{N-2a}{4})$, and second, that it reproduces the $T_{1,s}$ generated by (27)–(28) where all $Q_j(\theta)\big|_{j<N}$ are set to 1. For the vacuum state $P_\infty(\theta) = \frac{\theta^{N-1}}{(N-1)!}$.

In the gauge $T^{(L)}$, by contrast, we symmetrically choose $T^{(L)}_{0,s}(\theta) = T^{(L)}_{0,0}(\theta + s\frac{i}{2})$ and $T^{(L)}_{N,s}(\theta) = T^{(L)}_{N,0}(\theta - s\frac{i}{2})$, and we have

$$T^{(L)}_{a,s}(\theta) = i^{\frac{N(N-1)}{2}} \mathrm{Det}(c'_{j,k})_{1\le j,k\le N} \tag{54}$$

$$\text{where} \qquad c'_{j,k} = \overline{q_j}'\left(\theta + \frac{i}{2}\left(-s + a + 1 + \frac{N}{2} - 2k\right)\right) \quad \text{if } k \le a$$

$$\text{and} \qquad c'_{j,k} = q'_j\left(\theta + \frac{i}{2}\left(s + a + 1 + \frac{N}{2} - 2k\right)\right) \quad \text{if } k > a\,.$$

Now we will explain how this allows to generalize the large L solution of section 4 to any finite L.

24 The general solution doesn't assume that q's and $\bar{q}$'s are complex-conjugated. Nonetheless, our numerics has shown that at least for the states in the $U(1)$ sector, it is sufficient to restrict ourselves to the solutions where q's and $\bar{q}$'s are complex conjugated.

25 The present q-functions q_i are related to the functions Q_i in the Hasse diagram notation of [35].

7. Solution of the Y-system for PCF at a finite volume L

This section describes how to solve the finite volume Y-system by reducing it to a finite number of non-linear integral equations (NLIEs), that can be solved in its turn by iterative numerical methods.

We will focus on $U(1)$ sector states, although the method is in principle applicable to any excited state (see the discussion in subsection 9).

7.1. Definition of the jump densities

We propose here an ansatz for the finite size L solution by adding to the large L polynomial expressions (52)–(53) for q's certain terms decreasing for $\theta \to \pm\infty$ and exponentially small for $L \to \infty$ or $\theta \to \infty$: The finite L q_j's take thus the form

$$q_j(\theta) = \frac{\theta^{j-1}}{j-1!} + F_j(\theta) \qquad \text{when } j < N \text{ and } \mathrm{Im}(\theta) \le 0 \tag{55}$$

$$\overline{q_j}(\theta) = \frac{\theta^{j-1}}{j-1!} + \overline{F_j}(\theta) \qquad \text{when } j < N \text{ and } \mathrm{Im}(\theta) \ge 0 \tag{56}$$

$$q_N(\theta) = P(\theta) + F_N(\theta) \qquad \text{when } \mathrm{Im}(\theta) \le 0 \tag{57}$$

$$\overline{q_N}(\theta) = P(\theta) + \overline{F_N}(\theta) \qquad \text{when } \mathrm{Im}(\theta) \ge 0 \tag{58}$$

where

$$F_j(\theta) = \frac{1}{2i\pi} \int_{-\infty}^{\infty} \frac{f_j(\eta)}{\theta - \eta} \mathrm{d}\eta \qquad \text{when } \mathrm{Im}(\theta) < 0 \tag{59}$$

$$\overline{F_j}(\theta) = \frac{1}{2i\pi} \int_{-\infty}^{\infty} \frac{f_j(\eta)}{\theta - \eta} \mathrm{d}\eta \qquad \text{when } \mathrm{Im}(\theta) > 0 \tag{60}$$

and the polynomial P has the same degree as $P_\infty = \lim_{L\to\infty} P$ given by (53).[26] Note that for the vacuum state at finite L we have to choose[27] again $P = \frac{\theta^{N-1}}{(N-1)!}$. As a consequence of these definitions, we have

$$\overline{q_j}^{[+0]} - q_j^{[-0]} \equiv \lim_{\epsilon\to 0} \overline{q_j}^{[+\epsilon]} - q_j^{[-\epsilon]} = -f_j \tag{61}$$

so that f_j is actually the discontinuity (jump) between the functions q_j and $\overline{q_j}$ on the real axis.

Eqs. (55)–(58) define q_j only below the real axis and $\overline{q_j}$ above the real axis, so that the determinant only allows to compute $T_{a,s}$ inside the strip $\mathrm{Im}(\theta) \in [-\frac{N-2a}{4} - \frac{s+1}{2}, -\frac{N-2a}{4} + \frac{s+1}{2}]$. We can already see that these strips are the minimal strips to compute the Y functions on the

[26] The way we fix this polynomial will be explained in section 7.4, where the finite size Bethe equations are discussed.
[27] For vacuum, it would in principle be possible to set P to any polynomial of degree $N-1$. However, terms of lower degree than $N-1$ can be set to zero by operations on lines and columns of the determinant (49), and the normalization can be fixed to $P = \frac{\theta^{N-1}}{(N-1)!}$ at the price of changing the normalization of T-functions (a particular case of gauge transformation).

integration contour of equation (44), and we will see that it enables to compute the exact[28] energy of states in the $U(1)$ sector, at any length L.

The jump densities $f_j(\eta)$ are well defined on the real axis where they take only imaginary values, which follows from (61) and they are exponentially suppressed at large L or large $\cosh(\frac{2\pi}{N}\theta)$, as can be inferred from (9).

At the end of this subsection, let us comment on a slightly generalized version of our Wronskian solution of this section, now including the twisted, quasi-periodic boundary conditions on the wave function of the system. The twist matrix $g \in SU(N)$ can be chosen, without loss of generality, in a diagonal form: $g = \mathrm{diag}\{x_1, x_2, \cdots, x_N\}$ where the eigenvalues are unitary: $\bar{x}_j = \frac{1}{x_j}$, and $\prod_{j=1}^N x_j = 1$. Then the ansatz (55)–(58) will be modified[29]

$$q_j(\theta) = x_j^{i\theta} e^{F_j(\theta)} \qquad \text{when } 1 \le j < N \text{ and } \mathrm{Im}(\theta) \le 0 \tag{62}$$

$$\overline{q_j}(\theta) = x_j^{i\theta} e^{\overline{F_j}(\theta)} \qquad \text{when } 1 \le j < N \text{ and } \mathrm{Im}(\theta) \ge 0 \tag{63}$$

$$q_N(\theta) = P(\theta) x_N^{i\theta} e^{F_N(\theta)} \qquad \text{when } \mathrm{Im}(\theta) \le 0 \tag{64}$$

$$\overline{q_N}(\theta) = P(\theta) x_N^{i\theta} e^{\overline{F_N}(\theta)} \qquad \text{when } \mathrm{Im}(\theta) \ge 0 \tag{65}$$

with the same definition (60) for the functions $\bar{F}$, F (we can put $F_1 = \overline{F_1} = 0$). For the vacuum state, we should put $P(\theta) = 1$. In this case, in the limit $L \to \infty$ we obtain from the formula (49) that the T-function becomes a character of representation $\lambda = a^s$ of the twist matrix (up to the Vandermonde determinant $\Delta(x_1, \cdots, x_N)$). Note that it is not a trivial matter to reproduce in the untwisting limit $x_j \to 1$, $j = 1, 2, \ldots, N$ the ansatz (55)–(58): One has to do special rotations of the basis of q_j to arrive at the right answer.

The present article describes symmetric states (more specifically $U(1)$ sector states), for which there is a single twist matrix $g \in SU(N)$. But in general, there should be two independent $SU(N)$ twists due to the overall $SU(N) \times SU(N)$ symmetry. If we use a general $SU(N) \times SU(N)$ twist and break the symmetry of the state, then one would need two distinct sets of q-functions for the right and left wing, as argued in the discussion about non-symmetric states (in section 9). In that case, one twist appears in the parameterization (55)–(65) of the right wing, and another twist in the parameterization of the left wing.

7.2. *Relation to the analyticity of T functions*

From the ABA (41) and the finite size equation (20), we can see that

$$1 + Y_{a,0} \xrightarrow[\text{or } L \to \infty]{\theta \to \infty} 1 \qquad \text{when } |\mathrm{Im}(\theta)| < \frac{N}{4} \tag{66}$$

which means that $1 + Y_{a,0} = \frac{T_{a,0}^+ T_{a,0}^-}{T_{a+1,0} T_{a-1,0}}$ has a proper behavior in this strip, being a meromorphic function regular at infinity. On the other hand, when $|\mathrm{Im}(\theta)| = \frac{N}{4}$, $1 + Y_{a,0}$ oscillates at $Re(\theta) \to \infty$, and it diverges when, e.g., $|\mathrm{Im}(\theta)| \in [\frac{N}{4}, \frac{3N}{4}]$. By that reason we conclude that the

[28] Up to the precision of our numerical procedure solving these NLIE's.

[29] In this ansatz, one can either choose to write e^{F_j} or $1 + F_j$, it only amounts to a slight change of the functions F_j. What really differs with respect to (55)–(58) is the factor $x_j^{i\theta}$ and the fact that the polynomial term $\frac{\theta^{j-1}}{j-1!}$ is replaced by 1.

analyticity[30] strip of $1+Y_{a,0}=\frac{T^+_{a,0}T^-_{a,0}}{T_{a+1,0}T_{a-1,0}}$ is $\{\theta, |\mathrm{Im}(\theta)|<\frac{N}{4}\}$. From this we can identify the strips where the asymptotics (34) hold for $T_{a,s}$:

$$T_{0,0} \xrightarrow[L\cosh(\frac{2\pi\theta}{N})\to\infty]{} \varphi^{[-N/2]} \qquad \text{when } \mathrm{Im}(\theta)<\frac{N}{4} \tag{67}$$

$$T_{a,0}|_{0<a<N} \xrightarrow[L\cosh(\frac{2\pi\theta}{N})\to\infty]{} \varphi^{[+a-N/2]} \qquad \text{when } |\mathrm{Im}(\theta)|<\frac{N}{4}+\frac{1}{2} \tag{68}$$

$$T_{N,0} \xrightarrow[L\cosh(\frac{2\pi\theta}{N})\to\infty]{} \varphi^{[+N/2]} \qquad \text{when } \mathrm{Im}(\theta)>-\frac{N}{4}\,. \tag{69}$$

These conditions ensure the proper analyticity of $1+Y_{a,0}=\frac{T^+_{a,0}T^-_{a,0}}{T_{a+1,0}T_{a-1,0}}$, and the boundaries of the analyticity strips of each $1+Y_{a,0}$ are given by the boundaries of the analyticity strips of the corresponding T functions.[31]

Now, since we know that the T functions are described by Wronskian determinants, these analyticity strips suggest that

$$q_j \qquad \text{is analytic when} \qquad \mathrm{Im}(\theta)<1/2 \tag{70}$$

$$\overline{q_j} \qquad \text{is analytic when} \qquad \mathrm{Im}(\theta)>-1/2 \tag{71}$$

So the analyticity strip for q_j ends up at $\mathrm{Im}(\theta)=1/2$ which is reflected for instance in the fact that $T_{N-1,0}$ is not analytic when $\mathrm{Im}(\theta)>N/4+1/2$. This explains why $Y_{N-1,0}$ isn't analytic when $\mathrm{Im}(\theta)>N/4$.

Equations (70), (71) teach us that the analyticity domain is a bit bigger than what is necessary for (55)–(58). It tells us that in the definitions (59), (60), the contour can be shifted up to $\pm i/2$. In other words, the functions $f_j(\eta)$ are analytic on the strip $|\mathrm{Im}(\eta)|<1/2$.

It is noteworthy that even with these contour deformations, the determinant expressions (55)–(58) describe the function $T_{a,s}(\theta)$ inside the strip $\mathrm{Im}(\theta)\in\,]-\frac{N-2a}{4}-\frac{s}{2}-1, -\frac{N-2a}{4}+\frac{s}{2}+1[$, which is narrower than in equations (67), (69). But we will show that the relatively narrow strips given by this ansatz are sufficient to solve the Y-system and compute the energies.

7.3. Closed system of NLIEs

The gauge freedom (50), (51) can be used to impose $F_1(\theta)=\overline{F_1}(\theta)=0$, which leaves only $N-1$ independent densities to compute. Let us now see how $N-1$ equations on this densities can be obtained by imposing that the state is symmetric, i.e. that $Y_{a,-s}=Y_{a,+s}$. This requirement means that we can choose $T^{(L)}_{a,-s}=T_{a,s}$, which simplifies the Y-system equation for the middle node (16),[32] in the same manner as in [12].

Using this symmetry of the state and the boundary condition (48), equation (20) is reduced to:

[30] Note that we use the word "analyticity strip" to denote a domain where the $L\to\infty$ limit of Y- (resp. T- and q-) functions is a meromorphic (resp. holomorphic) function of θ.

[31] The analyticity strips for $T_{0,0}$ and $T_{N,0}$ can be chosen on a half plane thanks to an appropriate gauge.

[32] As a consequence, we are solving the Y-system under the following two constraints: $Y_{a,s}\sim e^{-Lp_a(\theta)\delta_{s,0}}\times \mathrm{const}_{a,s}$ on the one hand, and $T^{(L)}_{a,-1}=T_{a,1}$ one the other hand. This second constraint is specific to symmetric states (which includes the states in the $U(1)$ sector), such that $Y_{a,-s}=Y_{a,s}$.

$$Y_{a,0} = e^{-Lp_a} \frac{(T_{a,1})^2}{T_{a-1,0}T_{a+1,0}} \left(\frac{T_{0,0}^{[+N-a]} T_{N,0}^{[-a]}}{T_{0,0}^{[a-N]} T_{N,0}^{[+a]}} \right)^{\star K_N}, \tag{72}$$

or equivalently,

$$T_{a,-1}^{[a-N/2]} = e^{-Lp_a^{[a-N/2]}} T_{a,1}^{[a-N/2]} \left(\frac{T_{0,0}^{[+N/2]} T_{N,0}^{[-N/2]}}{T_{0,0}^{[2a-3N/2]} T_{N,0}^{[2a-N/2]}} \right)^{\star K_N}. \tag{73}$$

The reason why we chose such shifts in the relation (73) is that the l.h.s. has a determinant expression (49) where one has $c_{j,a} = \overline{q_j}^{[+0]}$ while $c_{j,a+1} = q_j^{[-0]}$. After subtracting one column from another in the determinant, there is a full column of $\overline{q_j}^{[+0]} - q_j^{[-0]} = -f_j$ which is exponentially small. That explains the exponential suppression of $T_{a,-1}$. Expanding the determinant w.r.t. these columns[33] gives the following linear system relating f_j's to $T_{a,-1}$'s:

$$T_{a,-1}\left(\theta - i\frac{N-2a}{4}\right) = \sum_j d_{a,j}(\theta) f_j(\theta) \tag{74}$$

$$\text{where } d_{a,j} = i^{\frac{N(N-1)}{2}} (-1)^{j+a+1} \frac{\det(c_{k,l})_{\substack{k\neq j\\ l\neq a}} + \det(c_{k,l})_{\substack{k\neq j\\ l\neq a+1}}}{2} \tag{75}$$

These $c_{k,l}$ are the coefficients of the determinant (49) defining $T_{a,-1}\left(\theta - i\frac{N-2a}{4}\right)$, and finally equations (72), (74) can be recast into

$$\sum_j d_{a,j}(\theta) f_j(\theta) = e^{-Lp_a(\theta - i\frac{N-2a}{4})} T_{a,1}^{[a-N/2]} \left(\frac{T_{0,0}^{[+N/2]} T_{N,0}^{[-N/2]}}{T_{0,0}^{[2a-3N/2]} T_{N,0}^{[-N/2+2a]}} \right)^{\star K_N}. \tag{76}$$

This is a closed system of equations on $\{f_j(\theta)\}_{\theta\in\mathbb{R}}$ because all coefficients $d_{a,j}$, and all T's can be computed out of f_j's through several convolutions.

The solution of the Y-system is therefore achieved by solving this system of $N-1$ equations on $N-1$ densities. The simple inversion of the linear system (74) brings (76) into the form

$$f_j(\theta) = H_j(\{f_k(\eta)\}_{\substack{k=2\dots N-1\\ \eta\in\mathrm{R}}}). \tag{77}$$

This H_j defines a contraction mapping in some vicinity of $f_j = 0$ when L is sufficiently large since it leads to an exponentially small $f_j(\theta)$. This implies that in some vicinity of $L=\infty$, the mapping H_j has a fixed point that can be found numerically through repeated iterations of H.

The way we solve Y-system is therefore simply the iteration of (77) and a good news is that, at least for $N=3$, even at very small L, this procedure seems, at least according to our numerics, to converge to a fix point of H_j, giving a complete solution of (77) and thus of the Y-system.

33 The two terms in (75) correspond to the fact that before expanding the determinant, we have added and subtracted columns to get one full column of $\overline{q_j}^{[+0]} - q_j^{[-0]} = -f_j$ and the other one of $\frac{\overline{q_j}^{[+0]} + q_j^{[-0]}}{2}$ (which corresponds to the principal value in (59), (60)).

7.3.1. Numerically workable form for the NLIE's

One difficulty of this numerical process is in computing the factor $\left(\frac{T_{0,0}^{[+N/2]}T_{N,0}^{[-N/2]}}{T_{0,0}^{[2a-3N/2]}T_{N,0}^{[-N/2+2a]}}\right)^{\star K_N}$ in the right hand side of (76). As we have already seen, the Wronskian formula (49) in terms of q_j's having cuts on the real axis allows to compute $T_{0,0}(\theta)$ only when $\mathrm{Im}(\theta) < -\frac{N}{4}+\frac{1}{2}$. So, for instance, $T_{0,0}(\theta + i\frac{N}{4})$ cannot be computed in this way when the spectral parameter θ is real. The denominator can nonetheless be computed if in the convolutions we shift appropriately both the argument of the kernel and of the T-functions

$$\left(\frac{1}{T_{0,0}^{[2a-3N/2]}T_{N,0}^{[-N/2+2a]}}\right)^{\star K_N} = \left(\frac{1}{T_{0,0}^{[-3N/2+a+1]}}\right)^{\star {K_N}^{[a-1]}} \left(\frac{1}{T_{N,0}^{[+N/2+a-1]}}\right)^{\star {K_N}^{[-N+a+1]}} \tag{78}$$

since $K_N(\theta)$ is regular when $\mathrm{Im}(\theta) \in [-\frac{N-1}{2}, \frac{N-1}{2}]$ and $a \in [1, N-1]$. Eq. (78) simply reflects the fact that if $k(\theta)$ is analytic for $\mathrm{Im}(\theta) \in [0, b/2]$, then for real θ, $\left(f^{[b]}\right)^{\star k} = f^{\star (k^{[b]})}$, $\forall f$.

The same idea, applied to the numerator, would give $\left(T_{0,0}(\theta + N\frac{i}{4})\right)^{\star K_N} = \left(T_{0,0}(\theta - N\frac{i}{4})\right)^{\star K_N^{[+N]}}$. But the equality fails because K_N has a pole at $i\frac{N-1}{2}$.

Instead, one can use the following relation

$$\left(T_{0,0}\left(\theta + N\frac{i}{4}\right)\right)^{\star K_N} = \frac{T_{0,0}(\theta - N\frac{i}{4}+\frac{i}{2})}{\left(T_{0,0}^{[+\frac{N}{2}-2]}T_{0,0}^{[+\frac{N}{2}-4]}\cdots T_{0,0}^{[-3\frac{N}{2}+2]}\right)^{\star K_N}} \tag{79}$$

$$= \frac{T_{0,0}(\theta - N\frac{i}{4}+\frac{i}{2})}{T_{0,0}(\theta - N\frac{i}{4}-\frac{i}{2})}\left(T_{0,0}^{[-3N/2]}\right)^{\star K_N} \tag{80}$$

which simply uses the fact that for a regular function f, $(\mathbf{\Pi}_N[f])^{\star K_N} = f$. This is true only up to a zero mode of $\mathbf{\Pi}_N$ which will be discussed in section 7.3.2.

Finally, the last factor in eq. (76) can be put into a numerically workable form by rewriting

$$\left(\frac{T_{0,0}^{[+N/2]}T_{N,0}^{[-N/2]}}{T_{0,0}^{[2a-3N/2]}T_{N,0}^{[-N/2+2a]}}\right)^{\star K_N}$$

$$= \frac{T_{0,0}^{[-N/2+1]}}{T_{0,0}^{[-N/2-1]}}\frac{T_{N,0}^{[N/2-1]}}{T_{N,0}^{[N/2+1]}}\left(\frac{T_{0,0}^{[-3N/2-a+1]}}{T_{0,0}^{[-3N/2+a+1]}}\right)^{\star K_N^{[a-1]}}\left(\frac{T_{N,0}^{[3N/2+N-a-1]}}{T_{N,0}^{[3N/2-N+a-1]}}\right)^{\star K_N^{[-N+a+1]}} \tag{81}$$

This will help us to transform eq. (76), once the appropriate zero mode is added, into a really closed system of NLIEs where the right hand side can indeed be computed by knowing the functions f_j only on the real axis.

7.3.2. χ_{CDD} factor

It is clear from the derivation of eq. (76), as well as of eqs. (79), (81) that they are fixed only up to a zero mode of the operator $\mathbf{\Pi}_N$. A zero mode Z therefore has to be added to (76), to get

$$\sum_j d_{a,j}(\theta) f_j(\theta) = Z\, e^{-L\cosh(\frac{2\pi}{N}(\theta - i\frac{N-2a}{4}))\frac{\sin(\frac{a\pi}{N})}{\sin(\frac{\pi}{N})}}\, T_{a,1}^{[a-N/2]}$$

$$\times \frac{T_{0,0}^{[-N/2+1]}}{T_{0,0}^{[-N/2-1]}} \frac{T_{N,0}^{[N/2-1]}}{T_{N,0}^{[N/2+1]}} \left(\frac{T_{0,0}^{[-3N/2-a+1]}}{T_{0,0}^{[-3N/2+a+1]}}\right)^{*K_N^{[a-1]}} \left(\frac{T_{N,0}^{[3N/2+N-a-1]}}{T_{N,0}^{[3N/2-N+a-1]}}\right)^{*K_N^{[-N+a+1]}} \tag{82}$$

Such zero mode can include for instance the factors $e^{-L\cosh(\frac{2\pi\theta}{N})}$ and χ_{CDD} from equation (42).

In the asymptotic limit ($L \to \infty$), the zero modes in equation (72) can be obtained by comparison with (41). In the same manner, the zero modes implicitly present in equation (81) can be computed in the asymptotic limit, by replacing $T_{a,0}$'s by their asymptotic values in terms of φ, see eq. (34), so that we can directly compute the zero mode Z when $L \to \infty$. We notice that, although both (76) and (81) are true up to a non-trivial zero mode, the zero mode in (82) happens to be[34]

$$Z = 1, \tag{83}$$

at least in the asymptotic limit!

Indeed, if we compare (82) with (41) (where $Y_{a,0} = \frac{T_{a,1}T_{a,-1}}{T_{a+1,1}T_{a-1,-1}}$ is expressed using (74)), we see that in the asymptotic limit we have

$$\begin{aligned} &Z \frac{T_{0,0}^{[-N/2+1]}}{T_{0,0}^{[-N/2-1]}} \frac{T_{N,0}^{[N/2-1]}}{T_{N,0}^{[N/2+1]}} \left(\frac{T_{0,0}^{[-3N/2-a+1]}}{T_{0,0}^{[-3N/2+a+1]}}\right)^{*K_N^{[a-1]}} \left(\frac{T_{N,0}^{[3N/2+N-a-1]}}{T_{N,0}^{[3N/2-N+a-1]}}\right)^{*K_N^{[-N+a+1]}} \\ &\sim \frac{\varphi^{[-N+1]}}{\varphi^{[-N+2a-1]}} \frac{\varphi^{[-N+1]}}{\varphi^{[-N+2a+1]}} \frac{1}{\mathbf{\Pi}_a \left[\left(S^{[a-N]}\right)^2 \chi_{CDD}^{[a-N]}\right]}, \end{aligned} \tag{84}$$

from where we will show that $Z_\infty = 1$, where Z_∞ denotes the asymptotic limit of Z, which can be extracted from (84). To this end, we can note that, as a direct consequence of (30), (38), (42), (67)–(69), we have $Z_\infty(\theta) = \prod_j Z_0(\theta - \theta_j)$, where Z_0 is the value of Z_∞ corresponding to $\varphi(\theta) = \theta$ (i.e. one single root at the origin). It is therefore sufficient to show that $Z_0 = 1$, i.e. to study equation (84) when $\varphi(\theta) = \theta$. In this case, we can easily list the zeroes and poles of the r.h.s. of (84): its zeroes are at positions $\frac{N-1}{2} + kN$, $\frac{3N+1}{2} - a + kN$, $-\frac{N-1}{2} - kN$ and $-\frac{N+1}{2} - a - kN$ (where $k \geq 0$ is an arbitrary non-negative integer) and its poles are at positions $\frac{N+1}{2} + kN$, $\frac{3N-1}{2} - a + kN$, $-\frac{N+1}{2} - kN$ and $-\frac{N-1}{2} - a - kN$.

We can then substitute the asymptotic limit (67)–(69) into the l.h.s. to find its analytic properties: one sees that the factor $\frac{T_{0,0}^{[-N/2+1]}}{T_{0,0}^{[-N/2-1]}} \frac{T_{N,0}^{[N/2-1]}}{T_{N,0}^{[N/2+1]}}$ reproduces the same zeros and poles as the r.h.s. at position $\pm\frac{N\pm1}{2}$, whereas the factors $(\ldots)^{\star K_N}$ are analytic when $-\frac{N-1}{2} - a < \mathrm{Im}(u) < \frac{N-1}{2} + N - a$. Hence we see that in the asymptotic limit, Z is analytic in the strip $-\frac{N-1}{2} - a < \mathrm{Im}(u) < \frac{N-1}{2} + N - a$, but as a zero-mode it is also $(N\,i)$-periodic. Moreover it behaves as a constant when $\mathrm{Re}(u) \to \infty$, so that Liouville theorem implies that Z_0 is a constant, hence (as a zero mode) it is equal to $e^{i\frac{2k\pi}{N}}$ for a given value of k. This factor can be

[34] Actually the right hand side of (82) is itself defined up to a factor of $e^{i\frac{2k\pi}{N}}$, because any $f^{\star K} = e^{K * \log f}$ is defined up to an $e^{2i\pi\int K}$ corresponding to the choice of the branch of the log. As a consequence, a more precise statement for (83) is $Z = e^{i\frac{2k\pi}{N}}$. k is chosen to reproduce (41), where the phase in (3) is chosen in such a way that one particle at rest ($\theta_1 = 0$) is a solution of the Bethe equation (43).

For states with zero momentum (like the mass gap and the vacuum), this extra phase can also be obtained by requiring a $\theta \to -\theta$ symmetry, which these states should exhibit.

absorbed into the ambiguity in the definition of the branch of the logarithm in the definition of $f^{\star K_N} = e^{\log f \star K_N}$ (see also footnote 34).

In the numerical solution of the Y-system we therefore assume that $Z = 1$ holds even at a finite size, i.e. that the analyticity structure of the zero modes is the same at finite L as at $L \to \infty$. We explicitly see that at $L \to \infty$, χ_{CDD} defined in (4) is taken into account in (82). In addition we can check that at finite size, we obtain Y functions having simple poles only.

7.4. Finite size Bethe equations

Bethe equations emerge in this procedure as a regularity requirement on the jump densities f_j's. Let us illustrate it for a general $U(1)$ state in the $SU(3)$ case, and also show why these finite L analogues of Bethe equations are equivalent, at large L, to the ABA Bethe equations on the roots of φ.

For such a state, the linear system (74) can be written as

$$\begin{pmatrix} A & B \\ -\overline{A} & -\overline{B} \end{pmatrix} \begin{pmatrix} f_2 \\ f_3 \end{pmatrix} = \begin{pmatrix} T_{1,-1}(\theta - i/4) \\ T_{2,-1}(\theta + i/4) \end{pmatrix} \tag{85}$$

where $A = \frac{i}{2}(q_3 + \overline{q_3}) - i\, q_3^{--}$ and $B = -\frac{i}{2}(q_2 + \overline{q_2}) + i\, q_2^{--}$.

Inverting the matrix $\begin{pmatrix} A & B \\ -\overline{A} & -\overline{B} \end{pmatrix}$, some singularity could occur at the zeroes of the function $\overline{A}B - A\overline{B}$, i.e. when the determinant is zero. If we want f_j's to be regular, we need the numerator to vanish at the same θ to cancel this pole. This gives the following finite size Bethe equation:

$$\text{If } \left(\overline{A}B - A\overline{B}\right)\Big|_{\tilde{\theta}_j} = 0 \text{ then } \begin{cases} T_{1,-1}(\tilde{\theta}_j - i/4)\overline{A}(\tilde{\theta}_j) = -T_{2,-1}(\tilde{\theta}_j + i/4)A(\tilde{\theta}_j) \\ T_{1,-1}(\tilde{\theta}_j - i/4)\overline{B}(\tilde{\theta}_j) = -T_{2,-1}(\tilde{\theta}_j + i/4)B(\tilde{\theta}_j) \end{cases} \tag{86}$$

One can notice that at such $\tilde{\theta}_j$ the two conditions in the r.h.s. are equivalent.

The claim that $\tilde{\theta}_j$ are a finite size analogue of the Bethe roots is supported by the fact that at large L, the roots of $\overline{A}B - A\overline{B}$ are precisely the Bethe roots. Indeed, at large L, $B \simeq 1$ and $A \simeq i(P - P^{--})$, giving $\overline{A}B - A\overline{B} \simeq i(P^{++} - P + P^{--} - P) = -i\varphi$. Moreover, we see from (45) that the second relation in the r.h.s. of (86) reduces then to the reality condition $\frac{\overline{T_{1,-1}(\theta_j - i/4)}}{T_{1,-1}(\theta_j - i/4)} = -1$. Using the leading-order large L expression of $Y_{a,0}$ in terms of S, eq. (41), we get at large L

$$T_{1,-1}(\theta - i/4) \simeq \frac{\varphi^{--}}{\varphi} \frac{\varphi + 2\varphi^{--}}{\mathcal{S}^{--}} e^{-L\cosh(\frac{2\pi}{3}(\theta - i/4))} \tag{87}$$

$$\text{where } \mathcal{S}(\theta) = \prod_j S_0^2(\theta - \theta_j)\check{\chi}_{CDD}(\theta - \theta_j)\,. \tag{88}$$

Using the fact that $\varphi(\theta_i) = 0$ at all Bethe roots θ_i, and dividing by the complex conjugate, the large L regularity requirement becomes

$$\left.\frac{(\varphi^{--})^2}{\varphi \mathcal{S}^{--}} \frac{\varphi}{(\varphi^{++})^2 \mathcal{S}^{++}}\right|_{\theta=\theta_i} e^{iL\sinh(\frac{2\pi}{3}\theta_j)} = -1\,. \tag{89}$$

Using the crossing relation, the left hand side becomes simply $\mathcal{S}(\theta_j)e^{iL\sinh(\frac{2\pi}{3}\theta_j)}$, so that the finite size regularity condition stated above is equivalent at large L to the asymptotic Bethe equations (43).

As a consequence, the iterative solution of the closed, finite size equations (82), should start from the expression (55), (58) where $P = P_\infty$ is given in terms of the asymptotic Bethe roots by (53), and then at each iteration, this polynomial is updated in order to incorporate this regularity condition.

7.4.1. Momentum number

In the asymptotic limit, one can introduce a notion of momentum number as follows: first one rewrites (43) in the form

$$\forall j, \quad e^{i\,L\,\sinh\frac{2\pi}{N}\theta_j + i\sum_{k\neq j} f(\theta_j-\theta_k)} = 1 \tag{90}$$

where the function

$$f(\theta) = -i\log(-\check{\chi}_{CDD}(\theta)S(\theta)^2) \tag{91}$$

is defined as a monotonous, continuous function, such that $f(0) = 0$. This allows to define the mode number of the particle j as the integer k such that $L\,\sinh\frac{2\pi}{N}\theta_j + \sum_{k\neq j} f(\theta_j-\theta_k) = 2\pi k$.

By contrast, at finite size, the regularity condition (86) involves the phase $-\frac{T_{1,-1}(\theta-i/4)\overline{B}(\theta)}{T_{2,-1}(\theta+i/4)B(\theta)}$. While there are several values of θ where this phase is equal to one, only a few of these values (one for each particle) are zeroes of $\overline{A}B - A\overline{B}$; the choice of these values defines the mode numbers at finite size.

To give a simple example, we can consider a state with a single Bethe root ($\mathcal{N} = 1$) and such that $L\,\sinh\frac{2\pi}{N}\theta_0 = 2\pi$ in the asymptotic limit (i.e. this state has momentum number 1). One can easily see that in the asymptotic limit the corresponding zero of $\overline{A}B - A\overline{B}$ is the second smallest positive zero of $\mathrm{Re}(T_{1,-1}(\theta - i/4)\overline{B}(\theta))$. Hence, at finite size, we recognize the state with mode number 1 as a state where the zero of $\overline{A}B - A\overline{B}$ is the second smallest positive zero of $\mathrm{Re}(T_{1,-1}(\theta - i/4)\overline{B}(\theta))$. To make sure that the iterative resolution algorithm does not "jump" from a state with given momentum number to another state, the momentum number has to be taken into account when the regularity condition (86) is enforced at every iteration.

7.4.2. $N > 3$ case

The same construction leads to finite size Bethe equations for any odd N. Like in equation (86) the number of regularity constraints at each zero of the determinant is apparently $N - 1$ but reduces to only *one* constraint: the cancellation of the projection of $\begin{pmatrix} T_{1,-1}(\theta - i(N-2)/4) \\ \vdots \\ T_{N-1,-1}(\theta + i(N-2)/4) \end{pmatrix}$ to the kernel of the matrix $d_{i,j}$ defining the linear system (74).

This procedure for finite-size Bethe equations was described here for odd N and for states having real Bethe roots in the asymptotic limit. The subtlety which arises when N is even, or for the states having, in the asymptotic limit, complexes of complex-conjugated Bethe roots, is that the zeroes of the determinant do not lie on the real axis but approximately on $\mathbb{R} \pm i/2$. The above procedure can in principle be applied anyway, but its interpretation is left to clarify because the regularity condition is imposed at the very boundary of the analyticity strip.

7.5. Numerical results

As seen in Fig. 4, this method allows to compute numerically the energies of excited states of the $U(1)$ sector for the whole physically interesting range of lengths L, from deep IR to deep

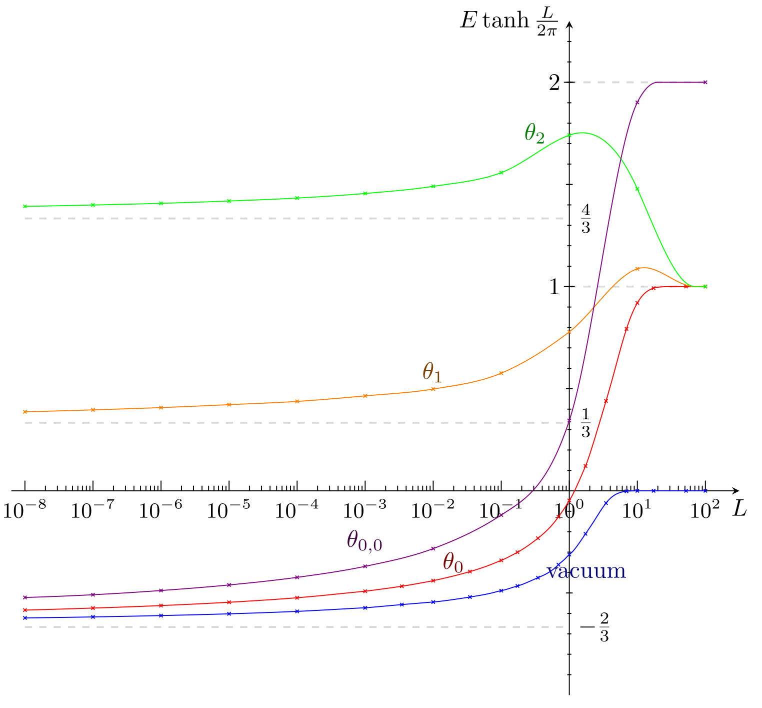

Fig. 4. Energies[35] of vacuum, of mass gap and of some excited states as functions of L, at $N = 3$. We see that in the $L \to \infty$ limit, E tends to the number of "particles" (i.e. Bethe roots), whereas in the conformal $L \to 0$ limit, $E \sim \frac{2\pi}{L}(-\frac{N^2-1}{12} + n)$, where n is the sum of the mode numbers of the "particles". The curves are interpolations from the numeric points (small crosses).

UV region. We can see that in the IR, $L \to \infty$ limit, the energies of individual states basically tend to the number of "particles" forming the state – the number of the Bethe roots θ_j: The vacuum energy tends to 0, while the energies of the states θ_0, θ_1 and θ_2 tend to 1, and the energy of θ_{00} tends to 2. In the conformal limit $L \to 0$, we will see that the behavior is defined by the "particle's" mode numbers: The energy goes to $\frac{2\pi}{L}(-\frac{N^2-1}{12} + n)$ where $N^2 - 1$ is the conformal central charge (the number of free bosonic fields of the model in this regime) and n is the total momentum mode number (see the discussion of IR and UV limits in the next section).

7.5.1. Numerical restrictions

As the length L is decreasing, the algorithm looks worse and worse converging, and the densities become more and more peaked around the endpoints of the distribution. By choosing a small enough interpolation step (the densities f_j are numerically defined by polynomial interpolation from a finite number of values), it was nevertheless possible to make the algorithm reasonably convergent for the considered states and lengths L, when $N = 3$. Decreasing further the interpolation step means increasing the computation time and the necessary amount of memory, which puts a practical limit to our precision and to the minimal length.

35 This figure shows the combination $E \tanh \frac{L}{2\pi}$, to make manifest the limit of E at large L, and of $E \frac{L}{2\pi}$ at small L.

Table 1
Numerical energies[36] for several $U(1)$ sector states at $N = 3$.

L	E_{vacuum}	E_{θ_0}	E_{θ_1}	E_{θ_2}	$E_{\theta_{0,0}}$
10^{-8}	$-3.909\ 10^{8}$	$-3.668\ 10^{8}$	$2.43\ 10^{8}$	$8.749\ 10^{8}$	$-3.28\ 10^{8}$
10^{-7}	$-3.8780\ 10^{7}$	$-3.606\ 10^{7}$	$2.55\ 10^{7}$	$8.791\ 10^{7}$	$-3.196\ 10^{7}$
10^{-6}	$-3.8366\ 10^{6}$	$-3.529\ 10^{6}$	$2.56\ 10^{6}$	$8.843\ 10^{6}$	$-3.066\ 10^{6}$
10^{-5}	$-3.7829\ 10^{5}$	$-3.427\ 10^{5}$	$2.65\ 10^{5}$	$8.914\ 10^{5}$	$-2.895\ 10^{5}$
10^{-4}	$-3.7077\ 10^{4}$	$-3.289\ 10^{4}$	$2.75\ 10^{4}$	$9.005\ 10^{4}$	$-2.661\ 10^{4}$
10^{-3}	$-3.5983\ 10^{3}$	$-3.088\ 10^{3}$	$2.92\ 10^{3}$	$9.146\ 10^{3}$	$-2.322\ 10^{3}$
10^{-2}	$-3.4206\ 10^{2}$	$-2.7629\ 10^{2}$	$3.13\ 10^{2}$	$9.365\ 10^{2}$	$-1.777\ 10^{2}$
10^{-1}	$-3.0715\ 10^{1}$	$-2.1393\ 10^{1}$	$3.62\ 10^{1}$	$9.788\ 10^{1}$	-7.439
1	$-1.9783\ 10^{0}$	$-2.993\ 10^{-1}$	4.93	11.031	2.180
10^{1}	$-1.0683\ 10^{-4}$	.9995	1.181	1.606	2.066
10^{2}	$-2.8\ 10^{-44}$	.999999	1.002	1.008	2.001

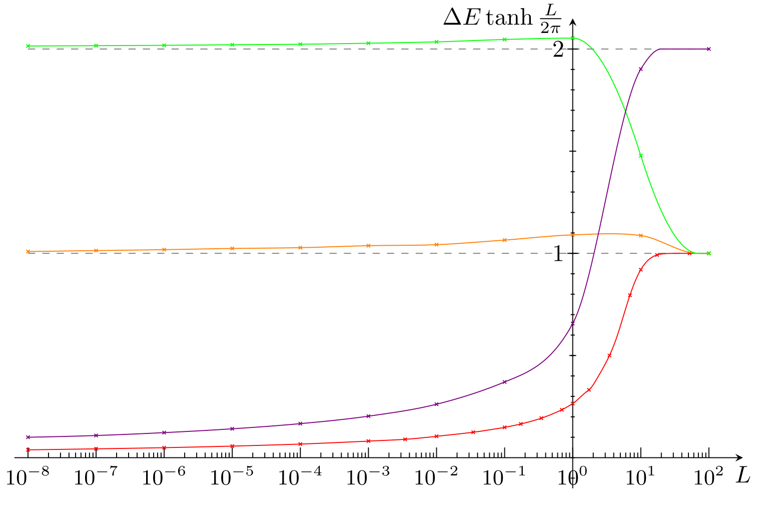

Fig. 5. Differences of energies, as functions of L, at $N = 3$. For low lying excited states, the combination $(E - E_{vacuum}) \tanh \frac{L}{2\pi}$ is plotted, as in Fig. 4.

Unfortunately, at $N \geq 4$ the calculations become heavier and with the size of interpolation steps we can afford our algorithm becomes instable already for L of order ~ 1 (which means we cannot really check, for instance, the conformal limit). At the moment we cannot say whether this instability has a physical meaning (like some symmetry breakdown, or some new type of singularity appearing) or whether it is just a numerical artifact, due to a poor numerical accuracy, or to the choice of the equations. For instance, it could be that the equation we iterate stops to correspond to a contraction mapping but still has a fixed point, and maybe even that, by rewriting slightly the functions, it could become a contraction again, and extracting its fixed point would be possible by iterations.

[36] In the table, the last digit (grayed out) is indicative and is not claimed to be accurate.

8. IR and UV limits

In this section, we will compute analytically the IR, finite size corrections to particular lowest lying states, as well as the UV, small size limit for a general state of the model. These results are very useful for checking our numerical data.

8.1. Leading order results at large L

The approach of this paper allows to compute the first exponential finite size correction, the so called Lüscher correction, to the energy at large L, as we will show now on a few examples.

8.1.1. Vacuum

The large L behavior of vacuum is given by the condition that

$$Y_{a,0}|_{\substack{L\to\infty \\ \text{Lüscher}}} = (T_{a,1})^2 e^{-Lp_a} \tag{92}$$

where $T_{a,1}$ is equal, according to the formulas (49), (52) and (53), to the binomial coefficient $\binom{N}{a}$. This is obtained from (41) where $\varphi = 1$, and can be plugged directly into (10) to get the energy to the leading order. For instance, if $N = 3$, one gets $E_{vacuum} \simeq -9\sqrt{\frac{2}{\pi L}}e^{-L}$. By construction, this expression fits well our numerical results when L is large enough.[37]

8.1.2. Mass gap at N = 3

When $N = 3$ it suffices to compute $Y_{1,0}$ to get the energy, because $Y_{2,0} = \overline{Y_{1,0}}$. Moreover the previous analysis shows that

$$Y_{1,0} = e^{-L\cosh(\frac{2\pi}{3}\theta)} \frac{(T_{1,1})^2}{T_{0,0}T_{2,0}} \frac{1}{S_0(\theta - 3\frac{i}{4})^2} \frac{\varphi(\theta - 3\frac{i}{4})}{\varphi(\theta + \frac{i}{4})} \frac{1}{\chi_{CDD}(\theta - 3\frac{i}{4})} \tag{93}$$

$$= e^{-L\cosh(\frac{2\pi}{3}\theta)} \frac{(3\theta - 5\frac{i}{4})^2}{\left(\theta + \frac{i}{4}\right)^2} \frac{1}{S_0(\theta - 3\frac{i}{4})^2} \frac{1}{\chi_{CDD}(\theta - 3\frac{i}{4})} \tag{94}$$

that enables to compute at large L the leading order value of the integral term in (46).

Unlike the vacuum case, we have to compute now the second term of (46) which is a bit tricky as it involves the position of the Bethe root. This position can be estimated by computing the densities to the leading order, to deduce the first correction to $T_{1,0}$ in order to solve the equation $T_{1,0}(\theta_0 + i/4) = 0$.

For the mass gap, this root should be at the origin, up to exponential corrections in L. Moreover, one can show[38] that $T_{1,0}(0+i/4) \sim \frac{i}{6} f_2(0) + i f_3(0) = \mathcal{O}(e^{-L\sqrt{3}/2})$, while $T'_{1,0}(0+i/4) \sim i$, so that $T_{1,0}(\theta_0 + i/4) = 0$ gives $\theta_0 \sim -\frac{1}{6} f_2(0) - f_3(0)$. Using the asymptotic expression for f_j's (which can be extracted by keeping only the leading order in $T_{a,s}$ and in $d_{a,j}$ in the

[37] When $L \geq 4$, the energy deviates from the asymptotic behavior precision by less than 10%, and this deviation quickly decreases when L increases.

[38] These large L expressions are obtained by neglecting integral terms in the determinant expression of $T_{1,0}$.

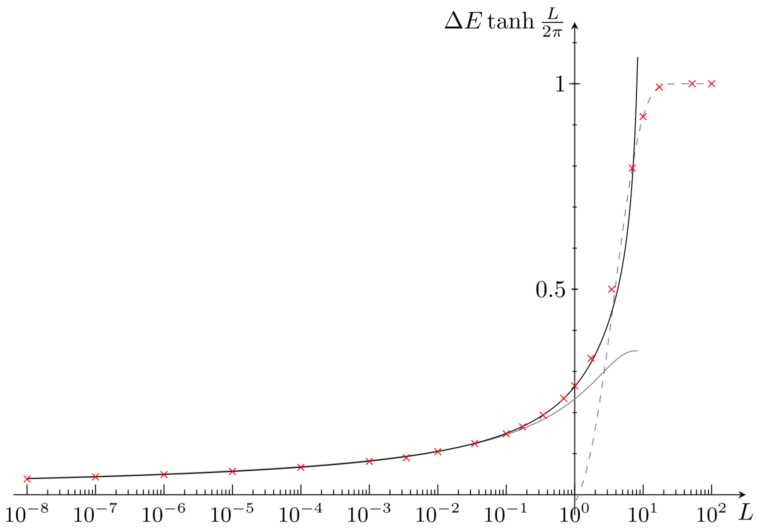

Fig. 6. Mass gap $\Delta E = E_{\theta_0} - E_{vacuum}$. The numeric results (crosses) are compared to the analytic Lüscher correction (95) for $E^{\text{mass gap}}_{L\to\infty}$ [dashed gray curve], to the 1-loop expression $\frac{L}{2\pi}[E_{\theta_0}(L) - E_0(L)] \approx \frac{8}{9}\frac{1}{\log\frac{c}{L}}$ [gray curve], and to the 2-loop expression $\frac{L}{2\pi}[E_{\theta_0}(L) - E_0(L)] \approx \frac{8}{9}\frac{1}{\log\frac{c}{L}+\frac{1}{2}\log\log\frac{c}{L}}$ [black curve] (101), where c is chosen as the best fit for the $L < 10^{-1}$ data.[39]

formula (76)), one gets $\theta_0 \sim \frac{i e^{-\sqrt{3}L/2}\Gamma\left(-\frac{1}{3}\right)^2\Gamma\left(\frac{2}{3}\right)^2}{\sqrt{3}\pi\Gamma\left(\frac{1}{3}\right)^2}$, so that the second term in (46), which is $\sinh\left(\frac{2\pi}{3}(\theta_0 - i/4)\right) - \sinh\left(\frac{2\pi}{3}(\bar{\theta}_0 + i/4)\right)$ can be computed at leading order.

That gives

$$E^{\text{mass gap}}_{L\to\infty} \simeq 1 - \left(\frac{32 e^{-\sqrt{3}L/2}\pi^3}{\Gamma\left(\frac{1}{3}\right)^6}\right) \tag{95}$$

which is in very good agreement the numerical results, as can be seen in Fig. 6.

Moreover, this expression (95) coincides exactly with the so-called μ-term [38,39], which is known to dominate the finite-size corrections in the presence of bound states.

8.2. Conformal limit at $L \to 0$

Let us start from the vacuum. At very small L, the effective coupling constant becomes very small $e_0^2(L) \simeq \frac{2\pi}{|\log L|}$ and we can linearize the field on the group manifold in the vicinity of $g(\sigma,\tau) = I$ as $g^{-1}\partial_\mu g \simeq i\,\partial_\mu A$, where $A(\sigma,\tau)$ is a Hermitian $N \times N$ traceless matrix field. The $SU(N)$ PCF model should become a 2D CFT of $N^2 - 1$ massless bosons: $R(L)$ is very big, the action (1) becomes

---

39 Explicitly we used the value $c = 44$ for the one-loop best-fit, and $c = 17$ for the two-loop best-fit.

$$\mathcal{S} = \frac{1}{2e_0^2(L)} \int \mathrm{d}\tau \int_0^L \mathrm{d}\sigma \sum_{\alpha=1}^{2} \mathrm{tr}[(\partial_\alpha A)^2] + O(e_0^4(L)). \tag{96}$$

In the ground state, the Casimir effect will dominate the limiting energy: $E_0 \simeq -\frac{\pi c}{6L} + O(1/\log^4(L^{-1}))$, with the central charge $c = N^2 - 1$, which gives $E_0 \frac{L}{2\pi} \simeq -\frac{N^2-1}{12}$.

The energies of excited states are

$$\frac{L}{2\pi} E_{\vec{n}_1\vec{n}_2\vec{n}_3\cdots}(L) \simeq -\frac{(N^2-1)}{12} + \sum_{k=1}^{\mathcal{N}} \sum_{\alpha=1}^{N^2-1} |n_k^{(\alpha)}| \tag{97}$$

where $\vec{n}_k = (n_k^{(1)}, n_k^{(2)}, \cdots, n_k^{(N^2-1)})$ are the momentum numbers of components of the k-th particle and $\mathcal{N}$ is the number of particles constituting the state. We see that the small L asymptotics of our plots are well described by this formula. The vacuum, and the states $\theta_0, \theta_{0,0}, \ldots$ have total momentum zero, and their energy satisfies $\frac{L}{2\pi} E(L) \simeq -\frac{(N^2-1)}{12}$. This formula explains well the fact that the corresponding plots in Fig. 4 converge, though slowly, as inverse logarithm of L, to $-(N^2-1)/12$. On the other hand, a state like θ_1 has the momentum number equal to 1 and $\frac{L}{2\pi} E(L) \simeq -\frac{(N^2-1)}{12} + 1$, etc.

The approximate behavior of the states θ_0, θ_{00}, etc., at very small L's can be explained by the fact that the quantum fields are dominated by their zero modes. Since the momentum modes are not excited the field $g(\sigma, \tau)$ does not depend on σ. The action and the Hamiltonian become:

$$\mathcal{S} \approx \frac{1}{2} \frac{L}{e_0^2(L)} \int d\tau \; \mathrm{tr}(g^{-1}\partial_\tau g)^2, \qquad \hat{H} = \frac{e_0^2(L)}{2L} \mathrm{tr}\hat{J}^2 \tag{98}$$

where the $g(\tau)$ represents the coordinate of a material point (a top) on the group manifold, and $\hat{J}$ is the corresponding angular momentum operator. The quantum mechanical spectrum of this system is well known: the quantum states are classified according to the irreducible representations of $su(N)$ characterized by highest weight with components $(m_1 \geq m_2 \geq \cdots \geq m_N)$ usually represented by a Young tableaux λ with N rows with the lengths m_j, $j = 1, \cdots, N$. The operator $\mathrm{tr}\hat{J}^2$ is nothing but the second Casimir operator with the well known eigenvalues, so that

$$\frac{L}{2\pi}(E_\lambda - E_0) \approx \frac{1}{4\pi} e_0^2(L)\, \mathrm{tr}\hat{J}^2 = \frac{e_0^2(L)}{4\pi} \sum_{k=1}^{N} r_k(r_k - 2k + N + 1) \tag{99}$$

where $r_k = m_k - \frac{1}{N}\sum_{j=1}^N m_j$.

We can use the two-loop expression for our length scale $L \ll 1$

$$\frac{L}{c} = \sqrt{\frac{4\pi}{N}} \frac{1}{e_0} e^{-\frac{4\pi}{Ne_0^2}}$$

where the constant c is defined by the renormalization scheme (corresponding to our TBA approach). We will use this constant as a fitting parameter in our numerical results. This gives for the two-loop running coupling: $\frac{4\pi}{Ne_0^2} = \log \frac{c}{L} + \frac{1}{2} \log\log \frac{c}{L}$.

For instance, for a state with only M real roots in the asymptotic limit (and without self-conjugated complexes of roots), we have $m_1 = M$, $m_{k\geq 2} = 0$, and hence

$$\frac{L}{2\pi}(E_{\theta\underbrace{\{0,0,\ldots,0\}}_{M\text{ times}}} - E_0) \approx \frac{e_0^2(L)}{4\pi N}(N-1)M(M+N)\,. \tag{100}$$

The 2-loop perturbative calculation of the mass gap $[E_{\theta_0}(L) - E_0(L)]$ for $L \ll 1$ was done in [40]. It was compared with the numerical results following from the TBA approach in [6] for $N = 2$. Here we cite this result only for the mass gap ($M = 1$), in the logarithmic approximation using the 2-loop result of [41,42]:

$$\frac{L}{2\pi}[E_{\theta_0}(L) - E_0(L)] \approx \frac{N^2-1}{N^2}\frac{1}{\log\frac{c}{L} + \frac{1}{2}\log\log\frac{c}{L}} \qquad (L \ll 1) \tag{101}$$

which is in the perfect agreement with (99), as well as with our numerics, as seen from Fig. 6. In this figure the gray and black curve show respectively the one and two-loop expressions of the mass gap when $N = 3$. The value of c used in this picture is chosen to fit the $L < 10^{-1}$ numeric data, and remarkably enough, the two-loop expression is reasonably close to the exact result up to $L \simeq 3$.

In principle, the three loop running coupling is also known in a certain scheme [43,44] but accounting for it will be beyond the accuracy of our numerics.

Formula (99) also gives a prediction for the state θ_{00} with two zero-momentum-particles, namely, for $N = 3$ we have $\frac{E_{\theta_{00}}(L)-E_0(L)}{E_{\theta_0}(L)-E_0(L)} \simeq \frac{5}{2}$. This result matches our numerics when L is smaller than 1 (see Fig. 5), up to the precision announced in Table 1.

Although the motivation of our approach was based on adding some terms, such as resolvents F_k in (55)–(58), correcting the infinite size solution, it reproduces correctly these conformal expressions, which shows that this description is not only accurate in some vicinity of $L = \infty$, but even in the conformal limit where L is very small. It proves that these terms were added by us into the ansatz (55)–(58) in a sufficiently general manner to describe the relevant exact solutions of the Y-system at any finite L.

9. Discussion

We have presented here, on the example of the $SU(N)$ principal chiral field model, a powerful and rather general approach to the study of finite volume spectrum of various integrable $1 + 1$ dimensional sigma-models. The approach continues the ideas of [12] where the method was proposed on the example of the $SU(2)$ PCF, but for $N > 2$ the method has to be seriously reconsidered due to many new physical features w.r.t. the $N = 2$ case. In particular, the presence of the bound state particles and the non-reality of the Bethe roots at finite L show a few qualitatively new features within our approach.

For virtually all integrable sigma models at a finite volume, the TBA-like approach initiated by Al. Zamolodchikov can be summarized in a very universal system of functional equations, the Y-system. The Y-system is equivalent to the famous Hirota equation – the Master equation of integrability describing in this case the integrable discrete dynamics with respect to a pair of "representational" variables, a, s and the spectral parameter (rapidity) θ. The boundary conditions for a, s are defined by the symmetry algebra of the model, whether as the analytic structure w.r.t. the θ variable is in general the most complicated issue, largely defining the dynamics of the model. However, in fact even the possible analyticity structures are greatly constrained by Hirota dynamics and by the symmetry algebra. It would be interesting to classify possible types of analyticity stemming from Hirota dynamics and some simple physical arguments (relativistic invariance, crossing, absence of certain singularities, etc.) related to the finite volume sigma models, similarly to the S-matrix bootstrap theory of Al. and A. Zamolodchikov valid only at infinite volume. This could lead to an interesting classification of sigma models themselves and possibly to the discovery of new integrable models. It would also help bypassing the standard TBA approach, poorly justified and, strictly speaking, valid only for the vacuum state.

In this paper, we managed to transform the finite volume spectral problem for one such relativistic σ-model, the $SU(N) \times SU(N)$ principal chiral field into a finite set of NLIEs. It was achieved by solving the underlying finite L Y-system in terms of Wronskian determinants of a finite number of Q-functions and parameterizing these Q-functions by $N-1$ densities correcting their large L asymptotics to any finite L.

Our work generalizes the analytic and numerical results of [12] to $N \geq 2$, and we could numerically check, at least when $N = 2, 3$, that this procedures solves the Y-system, and enables to compute energies for a wide range of lengths L, compatible with the UV conformal limit and the IR finite size (Lüscher) corrections. On the way, we conjectured a natural generalization of the energy formula for excited states for the $U(1)$ at finite L, to $N \geq 2$. This generalization appears to be unexpectedly non-trivial and looks different for even and odd N. The question of definition of the energy formula for excited states deserves a better understanding and hopefully the eventual derivation.

The analysis was done for $U(1)$ sector states, and it certainly can and should be generalized to any excited state, as was done in [12] for $N = 2$. To do this, one will have to understand the asymptotic terms and the structure of zeroes. In particular, some extra zeroes should appear in Y-functions which might affect the way the energy is computed by contour manipulation. Apart from that, the main difference with $U(1)$ sector should be that for non-symmetric states (i.e. when $Y_{a,s} \neq Y_{a,-s}$), it will be necessary to introduce $N-1$ densities for the right wing and $N-1$ densities for the left wing. One would have to write (20) as $2(N-1)$ different equations, by writing the left-hand side either as $\frac{T^{(R)}_{1,1} T^{(R)}_{1,-1}}{T^{(R)}_{2,0} T^{(R)}_{0,0}}$ or as $\frac{T^{(L)}_{1,1} T^{(L)}_{1,-1}}{T^{(L)}_{2,0} T^{(L)}_{0,0}}$. Our approach based on the Wronskian solution of Y-system should a priori still enable us to compute the energies of these states.

An interesting problem which our approach might help to solve is the planar $N \to \infty$ limit in PCF at finite L. This PCF model has a rich history of its comparison to QCD and it might provide an important example of exactly solvable $2+1$ dimensional bosonic string theory, similarly to the matrix quantum mechanical model of the $1+1$ dimensional, $c = 1$ non-critical string theory proposed and solved in [45]. The exact and explicit solution for this limit was given in the case of infinite volume L but in the presence of a specific "magnetic" fields [46]. The finite volume solution might provide a deeper understanding of 't Hooft limit in asymptotically free QFT's and even reveal some new physical phenomena, such as a possible large N phase transition at some L_c, in analogy with the Yang–Mills theory on the 2D sphere [47] (equivalent to the one-dimensional PCF). This, seemingly 2nd order, phase transition was already observed numerically in [48].

As concerns the numerics, our algorithm converges very well for any length when $N \leq 3$, but for $N \geq 4$ it is very unstable for small enough length L, already at $L \lesssim 1$ (which means for instance that we cannot really check the convergence to the conformal UV limit). Hopefully this instability has no direct physical meaning and is just a numerical artifact, due to a poor numeric accuracy or to the bad choice of the iteration procedure for our NLIEs. It would be good to compare our results with the high precision Monte-Carlo simulations of $SU(3)$ [41,42] for the mass gap as a function of the volume, but these papers are mostly concerned with reaching the infinite volume asymptotically free regime for the lattice PCF model with the torus, rather than cylindric boundary conditions.

We believe that this method of derivation of a finite system of NLIEs for integrable sigma models is general and powerful enough to work for much more complicated cases of AdS/CFT correspondence, such as the superstring on the $AdS_5 \times S^5$ background dual to $N = 4$ SYM theory, and the so called ABJM model where the Y-system was already discovered [15,49,50]. The Wronskian quasiclassical character [18] and even the full quantum solution of the Hirota dynamics for AdS_5/CFT_4 [19] are already available. The understanding of the very rich and complicated analyticity structure of Q-functions for short operators is of a great help for the derivation of the AdS/CFT NLIE.

Acknowledgements

The work of VK was partly supported by the ANR grants INT-AdS/CFT (BLAN-06-0124-03) and GranMA (BLAN-08-1-313695) and the grant RFFI-08-02-00287. We would like to thank B. Vicedo for the participation on an early stage of this work, M. Douglas, A. Hegedus, E. Sobko, A. Tsvelik, P. Wiegmann, A. Zabrodin for useful discussions, L. Hollo for carefully reading this version of the manuscript, and especially N. Gromov and P. Vieira for their constant attention and numerous important comments in the course of this work. VK also thanks Simons Center for Geometry and Physics (Stony Brook) and Nordita Institute (Stockholm) where a part of this work was done, for their kind hospitality.

References

[1] C. Destri, H.J. de Vega, Light cone lattices and the exact solution of chiral fermion and sigma models, J. Phys. A 22 (1989) 1329.
[2] Al.B. Zamolodchikov, Thermodynamic Bethe ansatz in relativistic models: scaling 3-state Potts and Lee–Yang models, Nucl. Phys. B 342 (1990) 695–720.
[3] V.V. Bazhanov, S.L. Lukyanov, A.B. Zamolodchikov, Quantum field theories in finite volume: excited state energies, Nucl. Phys. B 489 (1997) 487, arXiv:hep-th/9607099.
[4] P. Dorey, R. Tateo, Excited states by analytic continuation of TBA equations, Nucl. Phys. B 482 (1996) 639, arXiv:hep-th/9607167;
P. Dorey, R. Tateo, Anharmonic oscillators, the thermodynamic Bethe ansatz, and nonlinear integral equations, J. Phys. A 32 (1999) L419, arXiv:hep-th/9812211.
[5] D. Fioravanti, A. Mariottini, E. Quattrini, F. Ravanini, Excited state Destri–De Vega equation for sine-Gordon and restricted sine-Gordon models, Phys. Lett. B 390 (1997) 243, arXiv:hep-th/9608091.
[6] J. Balog, A. Hegedus, TBA equations for excited states in the $O(3)$ and $O(4)$ nonlinear sigma-model, J. Phys. A 37 (2004) 1881, arXiv:hep-th/0309009.
[7] A. Hegedus, Nonlinear integral equations for finite volume excited state energies of the $O(3)$ and $O(4)$ nonlinear sigma-models, J. Phys. A 38 (2005) 5345, arXiv:hep-th/0412125.
[8] V.V. Bazhanov, S.L. Lukyanov, A.B. Zamolodchikov, Integrable structure of conformal field theory, quantum KdV theory and thermodynamic Bethe ansatz, Commun. Math. Phys. 177 (1996) 381, arXiv:hep-th/9412229;
V.V. Bazhanov, S.L. Lukyanov, A.B. Zamolodchikov, Integrable structure of conformal field theory. III: The Yang–Baxter relation, Commun. Math. Phys. 200 (1999) 297, arXiv:hep-th/9805008.
[9] J. Teschner, On the spectrum of the sinh-Gordon model in finite volume, Nucl. Phys. B 799 (2008) 403, arXiv:hep-th/0702214.
[10] D. Fioravanti, M. Rossi, On the commuting charges for the highest dimension $SU(2)$ operator in planar $N = 4$ SYM, J. High Energy Phys. 0708 (2007) 089, arXiv:0706.3936;
L. Freyhult, A. Rej, M. Staudacher, A generalized scaling function for AdS/CFT, J. Stat. Mech. 0807 (2008) P07015, arXiv:0712.2743;
D. Bombardelli, D. Fioravanti, M. Rossi, Large spin corrections in $N = 4$ SYM $sl(2)$: still a linear integral equation, Nucl. Phys. B 810 (2009) 460, arXiv:0802.0027.

[11] A.M. Tsvelik, P.B. Wiegmann, Exact solution of the degenerate exchange model, J. Phys. C 15 (1982) 1707; A.M. Tsvelik, P.B. Wiegmann, The exact results for magnetic alloys, Adv. Phys. 32 (1983) 453.

[12] N. Gromov, V. Kazakov, P. Vieira, Finite volume spectrum of 2D field theories from Hirota dynamics, J. High Energy Phys. 0912 (2009) 060, arXiv:0812.5091.

[13] A. Kuniba, T. Nakanishi, J. Suzuki, Functional relations in solvable lattice models. 1: Functional relations and representation theory, Int. J. Mod. Phys. A 9 (1994) 5215, arXiv:hep-th/9309137.

[14] I. Krichever, O. Lipan, P. Wiegmann, A. Zabrodin, Quantum integrable models and discrete classical Hirota equations, Commun. Math. Phys. 188 (1997) 267, arXiv:hep-th/9604080;
A. Zabrodin, Discrete Hirota's equation in quantum integrable models, Int. J. Mod. Phys. B 11 (1997) 3125–3158, arXiv:hep-th/9610039;
A. Zabrodin, Hirota equation and Bethe ansatz, Teor. Mat. Fys. 116 (1998) 54–100, English translation: Theor. Math. Phys. 116 (1998) 782–819.

[15] N. Gromov, V. Kazakov, P. Vieira, Exact spectrum of anomalous dimensions of planar $N = 4$ supersymmetric Yang–Mills theory, Phys. Rev. Lett. 103 (2009) 131601, arXiv:0901.3753.

[16] D. Bombardelli, D. Fioravanti, R. Tateo, Thermodynamic Bethe ansatz for planar AdS/CFT: a proposal, J. Phys. A 42 (2009) 375401, arXiv:0902.3930;
N. Gromov, V. Kazakov, A. Kozak, P. Vieira, Exact spectrum of anomalous dimensions of planar $N = 4$ supersymmetric Yang–Mills theory: TBA and excited states, Lett. Math. Phys. 91 (2010) 265, arXiv:0902.4458;
G. Arutyunov, S. Frolov, Thermodynamic Bethe ansatz for the $AdS_5 \times S^5$ mirror model, J. High Energy Phys. 0905 (2009) 068, arXiv:0903.0141.

[17] N. Gromov, V. Kazakov, P. Vieira, Exact spectrum of planar $\mathcal{N} = 4$ supersymmetric Yang–Mills theory: Konishi dimension at any coupling, Phys. Rev. Lett. 104 (2010) 211601, arXiv:0906.4240.

[18] N. Gromov, V. Kazakov, Z. Tsuboi, $PSU(2, 2|4)$ character of quasiclassical AdS/CFT, J. High Energy Phys. 07 (2010) 097, http://dx.doi.org/10.1007/JHEP07(2010)097, arXiv:1002.3981.

[19] N. Gromov, V. Kazakov, S. Leurent, Z. Tsuboi, Wronskian solution for AdS/CFT Y-system, J. High Energy Phys. 1101 (2011) 155, arXiv:1010.2720.

[20] A.B. Zamolodchikov, A.B. Zamolodchikov, Factorized S-matrices in two dimensions as the exact solutions of certain relativistic quantum field models, Ann. Phys. 120 (1979) 253.

[21] B. Berg, M. Karowski, P. Weisz, V. Kurak, Factorized $U(N)$ symmetric S matrices in two-dimensions, Nucl. Phys. B 134 (1978) 125.

[22] P. Wiegmann, Exact factorized S matrix of the chiral field in two-dimensions, Phys. Lett. B 142 (1984) 173.

[23] B. Sutherland, A general model for multicomponent quantum systems, Phys. Rev. B 12 (1975) 3795.

[24] P.P. Kulish, N.Y. Reshetikhin, E.K. Sklyanin, Yang–Baxter equation and representation theory. 1, Lett. Math. Phys. 5 (1981) 393.

[25] T. Matsubara, A new approach to quantum statistical mechanics, Prog. Theor. Phys. 14 (1955) 351.

[26] P. Wiegmann, On the theory of nonabelian Goldstone bosons, in two dimensions; exact solution of the $SU(N) \times SU(N)$ nonlinear σ model, Phys. Lett. B 141 (1984) 217.

[27] A.M. Polyakov, P.B. Wiegmann, Theory of nonabelian Goldstone bosons in two dimensions, Phys. Lett. B 131 (1983) 121.

[28] L.D. Faddeev, N.Y. Reshetikhin, Integrability of the principal chiral field model in $(1 + 1)$-dimension, Ann. Phys. 167 (1986) 227.

[29] C.N. Yang, C.P. Yang, One-dimensional chain of anisotropic spin–spin interactions, Phys. Rev. 147 (1966) 303; C.N. Yang, C.P. Yang, J. Math. Phys. 10 (1969) 1115.

[30] V.A. Fateev, A.B. Zamolodchikov, Integrable perturbations of $Z(N)$ parafermion models and $O(3)$ sigma model, Phys. Lett. B 271 (1991) 91.

[31] J. Balog, A. Hegedus, TBA equations for the mass gap in the $O(2r)$ non-linear sigma-models, Nucl. Phys. B 725 (2005) 531, arXiv:hep-th/0504186.

[32] A. Hegedus, Nonlinear integral equations for the finite size effects of RSOS and vertex-models and related quantum field theories, Nucl. Phys. B 732 (2005) 463, arXiv:hep-th/0507132.

[33] Z. Tsuboi, Analytic Bethe ansatz and functional equations for Lie superalgebra $sl(r + 1|s + 1)$, J. Phys. A 30 (1997) 7975, arXiv:0911.5386.

[34] V. Kazakov, A. Sorin, A. Zabrodin, Supersymmetric Bethe ansatz and Baxter equations from discrete Hirota dynamics, Nucl. Phys. B 790 (2008) 345, arXiv:hep-th/0703147;
A. Zabrodin, Backlund transformations for difference Hirota equation and supersymmetric Bethe ansatz, Theor. Math. Phys. 155 (2008) 567–584, arXiv:0705.4006;
V. Kazakov, P. Vieira, From characters to quantum (super)spin chains via fusion, J. High Energy Phys. 10 (2008) 050, arXiv:0711.2470.

[35] Z. Tsuboi, Solutions of the T-system and Baxter equations for supersymmetric spin chains, Nucl. Phys. B 826 (2010) 399, arXiv:0906.2039.
[36] I. Cherednik, An analogue of character formula for Hecke algebras, Funct. Anal. Appl. 21 (2) (1987) 94–95 (translation: pp. 172–174).
[37] V. Bazhanov, N. Reshetikhin, Restricted solid on solid models connected with simply based algebras and conformal field theory, J. Phys. A 23 (1990) 1477.
[38] M. Lüscher, Volume dependence of the energy spectrum in massive quantum field theories. 1. Stable particle states, Commun. Math. Phys. 104 (1986) 177;
M. Luscher, Volume dependence of the energy spectrum in massive quantum field theories. 2. Scattering states, Commun. Math. Phys. 105 (1986) 153.
[39] T.R. Klassen, E. Melzer, On the relation between scattering amplitudes and finite size mass corrections in QFT, Nucl. Phys. B 362 (1991) 329.
[40] D.S. Shin, A determination of the mass gap in the $O(n)$ sigma-model, Nucl. Phys. B 496 (1997) 408, arXiv:hep-lat/9611006;
D.S. Shin, Correction to four-loop RG functions in the two-dimensional lattice $O(n)$ sigma-model, Nucl. Phys. B 546 (1999) 669, arXiv:hep-lat/9810025.
[41] G. Mana, A. Pelissetto, A.D. Sokal, Asymptotic scaling in the two-dimensional $SU(3)$ sigma model at correlation length 4×10^5, Phys. Rev. D 54 (1996) 1252, arXiv:hep-lat/9602015.
[42] G. Mana, A. Pelissetto, A.D. Sokal, Multigrid Monte Carlo via XY embedding. 2. Two-dimensional $SU(3)$ principal chiral model, Phys. Rev. D 55 (1997) 3674, arXiv:hep-lat/9610021.
[43] P. Rossi, E. Vicari, Two-dimensional $SU(N) \times SU(N)$ chiral models on the lattice, Phys. Rev. D 49 (1994) 1621, arXiv:hep-lat/9307014;
P. Rossi, E. Vicari, Phys. Rev. D 55 (1997) 1698.
[44] P. Rossi, E. Vicari, Two-dimensional $SU(N) \times SU(N)$ chiral models on the lattice. 2. The Green's function, Phys. Rev. D 49 (1994) 6072, arXiv:hep-lat/9401029;
P. Rossi, E. Vicari, Phys. Rev. D 50 (1994) 4718;
P. Rossi, E. Vicari, Phys. Rev. D 55 (1997) 1698.
[45] V.A. Kazakov, A.A. Migdal, Recent progress in the theory of noncritical strings, Nucl. Phys. B 311 (1988) 171.
[46] V.A. Fateev, V.A. Kazakov, P.B. Wiegmann, Principal chiral field at large N, Nucl. Phys. B 424 (1994) 505, arXiv:hep-th/9403099.
[47] M.R. Douglas, V.A. Kazakov, Large N phase transition in continuum QCD in two-dimensions, Phys. Lett. B 319 (1993) 219, arXiv:hep-th/9305047.
[48] M. Campostrini, P. Rossi, E. Vicari, Large N phase transition in lattice 2-d principal chiral models, Phys. Rev. D 52 (1995) 395, arXiv:hep-lat/9412102.
[49] D. Bombardelli, D. Fioravanti, R. Tateo, TBA and Y-system for planar AdS_4/CFT_3, Nucl. Phys. B 834 (2010) 543, arXiv:0912.4715.
[50] N. Gromov, F. Levkovich-Maslyuk, Y-system, TBA and quasi-classical strings in $AdS_4 \times CP_3$, J. High Energy Phys. 1006 (2010) 088, arXiv:0912.4911.